Mathematical Biosciences and Engineering

http://www.aimspress.com/journal/MBE

MBE, 23(5): 1461–1500.
DOI: 10.3934/mbe.2026054
Received: 05 December 2025
Revised: 18 February 2026
Accepted: 09 March 2026
Published: 14 April 2026

Research article

Modeling the effects of trait–mediated dispersal on coexistence of two species: Competition and non–consumptive predator–prey

Ananta Acharya[1], Emily Cosgrove[2], James T. Cronin[3], Jerome Goddard II[2,*], Eddie Lindsey[2], Amila Muthunayake[4], Dustin Nichols[5] and Ratnasingham Shivaji[6]

[1] Department of Mathematical Sciences, Eastern New Mexico University, Portales, NM 88130, USA

[2] Department of Mathematics, Auburn University Montgomery, Montgomery, AL 36124, USA

[3] Department of Biological Sciences, Louisiana State University, Baton Rouge, LA 70803, USA

[4] Department of Mathematics, Weber State University, Ogden, UT 84408, USA

[5] Department of Mathematical Sciences, High Point University, High Point, NC 27262, USA

[6] Department of Mathematics and Statistics, University of North Carolina at Greensboro, Greensboro, NC 27412, USA

* **Correspondence:** Email: jgoddard@aum.edu; Tel: +13342443023; Fax: +13343943826.

Abstract: Fragmentation and loss of habitat owing to increased human activity are major drivers of species extinctions and declining global biodiversity. In ecological communities, trait–mediated indirect effects are frequently observed and can influence population dynamics as strongly, possibly even more strongly, than direct effects. However, few studies have focused on trait–mediated behavior such as trait–mediated dispersal, in which the dispersal patterns are altered by the presence of an interacting species. Moreover, little is known about how trait–mediated dispersal interacts with habitat fragmentation and loss to affect the coexistence of interacting species. Here, we explore the consequences of both trait–mediated dispersal and fragmentation/loss on coexistence in a system consisting of two competing species or a predator and its prey. By assuming that the density–mediated effects are negligible, we isolate the role of trait–mediated effects. Our results show that the combined influence of fragmentation and trait–mediated dispersal can substantially reshape the population dynamics and species coexistence outcomes.

Keywords: habitat fragmentation; trait–mediated dispersal; reaction diffusion model; competition; predator–prey; dead zone; founder control

1. Introduction

Interspecific interactions such as between competitors or predators and their prey crucially affect populations both in direct ways (e.g., density–mediated effects), and in indirect ways (e.g., trait–mediated effects). In the literature, direct effects typically receive more attention. For example, predator–prey studies are often concerned with rates of prey consumption by a predator and how that affects prey density (a density–mediated effect), ignoring indirect effects such as the influence of the predator on the phenotype of the surviving prey (see, e.g., [1–3]). In the review paper [1], several examples of trait–mediated behavior are given. One example, found in [4], examined the interaction of spiders and grasshoppers in a field. The authors observed the amount of grasshopper movement, the patterns of movement, and total activity time in response to the presence or absence of spider predators. To isolate the trait–mediated effect (e.g., fear), from the density–mediated effect (i.e., consumption of prey), the spiders had their chelicerae glued together. It was found that grasshoppers had reduced activity time and there was a significant diet shift from grass to herbs (which may also indicate a habitat shift) under the threat of predation. Under such conditions, we refer to this interaction as a non-consumptive predator–prey or trait–mediated predator–prey effect. The authors in [1] have made a case that ecological communities are full of indirect trait–mediated effects arising from mechanisms such as phenotypic plasticity, and these indirect effects are expected to strongly contribute to phenomena that would traditionally be attributed to density–mediated effects (see, e.g., [1, 2, 5]).

Population dynamics can be significantly affected by trait–mediated behavioral responses to other species (see [1, 6]). An example of such a behavioral response is trait–mediated dispersal, where an organism changes its dispersal patterns due to the presence of another species. This change can, in turn, modify population dynamics and species interactions (see, e.g., [7]). In the predator–prey context, this idea has been studied (though only scarcely) where an increased predation risk (i.e., fear) was shown to increase prey emigration rates. The authors in [8] found evidence of predator–induced emigration in a spider–planthopper system. They concluded that at high predator density, predator–induced emigration had a greater impact on the prey's density than consumption (see also [9–11]).

Loss and fragmentation of habitats are a major driver of species extinctions and declining biodiversity worldwide and have been greatly exacerbated by human activities over the past few centuries (see, e.g., [12–15]). Fragmentation creates landscape-level spatial heterogeneity, which has a tremendous influence on the population dynamics of resident species. Due to the increased susceptibility of the resident species to edge effects between remnant habitat patches and the lower quality "matrix" surrounding these focal patches, species abundance often declines [16–18]. Matrix composition and hostility can also have profound effects on the coexistence of interacting species, such as the reversal of dominance in competing species (see, e.g., [18–20]).

In this paper, we explore effects of trait–mediated dispersal on the coexistence of two species in a competitive context and a predator–prey context. In an analog of the empirical study [4] where the authors isolated the trait–mediated effect by removing the consumptive effects of the predator (gluing the spider's mouthparts together), we consider a theoretical system that can either model competition or predator–prey dynamics but where consumptive effects are assumed to be negligible. In this way, we will be able to isolate the dynamic effects of the indirect trait–mediated effects from those of the direct effects and draw more general conclusions regarding the trait–mediated dispersal mechanism.

We assume that both organisms inhabit the same patch located in a landscape and are surrounded by a hostile matrix. Both organisms grow according to logistic growth, and their movement is assumed to follow an unbiased random walk both in the patch and in the matrix. At the patch–matrix interface, a biased random walk is assumed, where the probability of an organism remaining inside the patch is dependent on the other organism's density, i.e., density-dependent emigration (DDE) (see [21] for a review of empirical DDE studies). In the competitive context, both organisms are assumed to exhibit positive DDE (+DDE), where their emigration is an increasing function of their competitor's density. In the predator–prey context, the prey's emigration is assumed to follow a +DDE relationship with respect to predator density, modeling fear of the presence of the predator, whereas the predator's emigration is assumed to follow a negative DDE (-DDE) relationship with respect to the prey's density modeling an attraction of the predator to prey. The effects of habitat fragmentation are integrated into the modeling framework by certain parameters that measure patch size and effective matrix hostility towards a particular organism. The overall modeling approach is based on a system of reaction diffusion equations and is only a caricature designed to explore the effects of trait–mediated dispersal and habitat fragmentation on the coexistence of the organisms. The model is not intended to be a detailed description of any particular animal system. A similar system was used by the authors in [22] for a system of two mutualists where both organisms exhibited -DDE with respect to the other organism's density, and in [23] for a predator–prey system where the prey responded by increasing its emigration in the presence of the predator but where the predator emigrated independent of the prey's density.

We provide the modeling framework in Section 1.1 and our main results in Section 2. In Section 3, we present some important mathematical preliminaries that will be used in proving our main results, which are given in Section 4. Finally, in Section 5, we give some overall implications of our findings.

1.1. Modeling framework

In this model, $(u(t,x), v(t,x))$ represents the normalized density (i.e., the carrying capacity is equal to one) of two different populations inhabiting the patch $\Omega_0 = \{\ell x : x \in \Omega\}$ with a patch size $\ell > 0$, $\Omega = (0,1)$, or $\Omega \subset \mathbb{R}^n$ having a unit measure (e.g., if $n = 2$, then the area of Ω is one) and a smooth boundary with $n = 2, 3$. The patch is surrounded by a hostile matrix, denoted $\Omega_M = \mathbb{R}^n \backslash \overline{\Omega}_0$. We also denote the boundary of Ω_0 by $\partial\Omega_0$. Here, the variable t represents time and x represents the spatial location within the patch. Following the derivation given in [24], the model is then

$$\begin{cases} u_t = D_1 \Delta u + r_1 u(1-u); \ t > 0, x \in \Omega_0 \\ v_t = D_2 \Delta v + r_2 v(1-v); \ t > 0, x \in \Omega_0 \\ u(0,x) = u_0(x); \ x \in \Omega_0 \\ v(0,x) = v_0(x); \ x \in \Omega_0 \\ D_1 \alpha_1(v) \frac{\partial u}{\partial \eta} + S_1^*[1-\alpha_1(v)]u = 0; \ t > 0, x \in \partial\Omega_0 \\ D_2 \alpha_2(u) \frac{\partial v}{\partial \eta} + S_2^*[1-\alpha_2(u)]v = 0; \ t > 0, x \in \partial\Omega_0, \end{cases} \tag{1.1}$$

where $D_i > 0$ represents the patch diffusion rate, $r_i > 0$ is the patch intrinsic growth rate, $u_0(x)$ and $v_0(x)$ the initial population density distributions in the patch, and $\alpha_i : [0,\infty) \to [0,1]$ are smooth functions representing the probability of an individual remaining in the patch upon reaching the boundary ($i = 1$ for u and $i = 2$ for v). Notice that $\alpha_1(v)$ and $\alpha_2(u)$ encode u and v's response to the other species,

respectively. In the case that α_i is an increasing function of the other species' density, this would encode attraction behavior (e.g., one competitor using the density of its competitor as a measure of habitat quality), whereas if α_i is a decreasing function, that would encode repulsion behavior (e.g., the prey attempting to avoid a predator or a species avoiding its predator due to overcrowding). The term $\frac{\partial}{\partial \eta}$ denotes the outward normal derivative operator. Here, the parameter $S_i^* \geq 0$ is a measure of the hostility of the matrix towards the organism, has the units $\frac{\text{length}}{\text{time}}$, and can assume different forms depending upon the patch–matrix interface assumptions (see [24]). The emigration rate then is modeled as $1 - \alpha_i$ and can be encoded to model a given relationship between density and the emigration rate by selecting appropriate values of α_i (see, [22, 23, 25–30]).

We note that if $\alpha_i \equiv 0$, then the boundary is absorbing; i.e., all individuals that reach the boundary will emigrate, whereas if $\alpha_i \equiv 1$, then the boundary is reflecting, i.e., the emigration rate is zero. Notice that in this derivation, organisms may exit the patch, spend some time in the matrix, and then later return to the patch. As noted in [24], the model (1.1) will exactly capture the dynamics of the study system in the case of a spatially one-dimensional patch in the sense that steady states of (1.1) and their stability properties will be exactly the same as those of the study system, while providing a reasonable approximation of the study system in the case of a simply connected, convex patch in two or three dimensions.

We now introduce a standard scaling, $\tilde{x} = \frac{x}{\ell}$ & $\tilde{t} = r_1 t$. After applying this scaling and dropping the tilde, (1.1) becomes

$$\begin{cases} u_t = \frac{1}{\lambda}\Delta u + u(1-u); \ t > 0, x \in \Omega \\ v_t = \frac{D_0}{\lambda}\Delta v + r_0 v(1-v); \ t > 0, x \in \Omega \\ u(0,x) = u_0(x); \ x \in \Omega \\ v(0,x) = v_0(x); \ x \in \Omega \\ \frac{\partial u}{\partial \eta} + \sqrt{\lambda} g(v)u = 0; \ t > 0, x \in \partial\Omega \\ \frac{\partial v}{\partial \eta} + \sqrt{\lambda} h(u)v = 0; \ t > 0, x \in \partial\Omega, \end{cases} \tag{1.2}$$

with the corresponding steady–state equations

$$\begin{cases} -\Delta u = \lambda u(1-u); \ \Omega \\ -\Delta v = \lambda r v(1-v); \ \Omega \\ \frac{\partial u}{\partial \eta} + \sqrt{\lambda} g(v)u = 0; \ \partial\Omega \\ \frac{\partial v}{\partial \eta} + \sqrt{\lambda} h(u)v = 0; \ \partial\Omega \end{cases} \tag{1.3}$$

where $\lambda = \frac{r_1 \ell^2}{D_1}$, $r_0 = \frac{r_2}{r_1}$, $D_0 = \frac{D_2}{D_1}$, $r = \frac{r_0}{D_0}$, $g(v) = \frac{S_1^*}{\sqrt{r_1 D_1}} \frac{1-\alpha_1(v)}{\alpha_1(v)}$, and $h(u) = \frac{S_2^*}{\sqrt{r_1 D_1 D_0}} \frac{1-\alpha_2(u)}{\alpha_2(u)}$ are all unitless. Thus, for a fixed r_1, r_2, D_1, D_2, the composite parameter λ is proportional to the square of the patch size, $g(0)$ represents the effective matrix hostility towards u, and $h(0)$ represents the effective matrix hostility towards v. Moreover, r can be written as $r = \frac{\frac{r_2}{D_2}}{\frac{r_1}{D_1}}$ and interpreted as a means to compare the two species by the growth-to-diffusion ratio, defined as the ratio of the patch intrinsic growth to the patch diffusion rate. Thus, (1) if $r = 1$, then both growth-to-diffusion ratios are the same; (2) if $r > 1$, then v's growth-to-diffusion ratio is greater than u's growth-to-diffusion ratio; and (3) if $r < 1$, then u's ratio is greater than v's.

2. Main results

We first present some results regarding certain eigenvalue problems that are necessary for the statement of our main results. The proceeding subsections then explore our main results in the case of trait–mediated competition and non–consumptive predator–prey. In all bifurcation diagram legends, we use *u-independent* (blue curve) and *v-independent* (red curve) to indicate the scenario where each species exists independently in the patch, whereas *u in presence of v* (green curve) and *v in presence of u* (purple curve) indicate the scenario where each species is in the presence of the other. We also include the corresponding emigration probability curves for both species, where the orange curve is for u and the cyan curve is for v.

2.1. Eigenvalue problems

We first recall the following eigenvalue problem studied in [31] whose principal eigenvalue is related to the minimum patch size for a species:

$$\begin{cases} -\Delta\phi = RE\phi; \ \Omega \\ \frac{\partial\phi}{\partial\eta} + \gamma\sqrt{E}\phi = 0; \ \partial\Omega, \end{cases} \tag{2.1}$$

where R and γ are positive parameters. There, it was shown that for a fixed R and γ, (2.1) has a positive principal eigenvalue $E_1(R,\gamma)$ with the corresponding normalized eigenfunction $\phi(x) > 0; \ \overline{\Omega}$. Moreover, when R is fixed, E_1 is increasing in γ, and when γ is fixed, E_1 is decreasing in R. These properties will aid us in establishing when u or v has a smaller minimum patch size requirement with the other species absent from the patch.

Now, we consider (1.3) in the cases when one population is present and the other is absent. First, for u being present and v being absent, (1.3) becomes

$$\begin{cases} -\Delta w_1 = \lambda w_1(1 - w_1); \ \Omega \\ \frac{\partial w_1}{\partial\eta} + \sqrt{\lambda}g(0)w_1 = 0; \ \partial\Omega \end{cases} \tag{2.2}$$

whereas, when v is present and u is absent, (1.3) becomes

$$\begin{cases} -\Delta w_2 = \lambda r w_2(1 - w_2); \ \Omega \\ \frac{\partial w_2}{\partial\eta} + \sqrt{\lambda}h(0)w_2 = 0; \ \partial\Omega. \end{cases} \tag{2.3}$$

As shown in [31] and [24], the solution structure of (2.2) and (2.3) can be completely determined by consideration of the eigenvalue problems, respectively

$$\begin{cases} -\Delta\phi = (\lambda + \sigma)\phi; \ \Omega \\ \frac{\partial\phi}{\partial\eta} + \sqrt{\lambda}g(0)\phi = 0; \ \partial\Omega, \end{cases} \tag{2.4}$$

and

$$\begin{cases} -\Delta\phi = (\lambda r + \sigma)\phi; \ \Omega \\ \frac{\partial\phi}{\partial\eta} + \sqrt{\lambda}h(0)\phi = 0; \ \partial\Omega. \end{cases} \tag{2.5}$$

We note that together, (2.4) and (2.5) comprise the linearization of (1.3) around $(0, 0)$. Let $\sigma_1 = \sigma_1(\Omega, \lambda, g(0))$ and $\sigma_2 = \sigma_2(\Omega, \lambda, r, h(0))$ be the principal eigenvalues, and let ϕ_1 and $\phi_2 > 0;\ \overline{\Omega}$ be the corresponding normalized eigenfunctions of (2.4) and (2.5), respectively. Notice that $\sigma_1 < 0$ (which will occur whenever $\lambda > E_1(1, g(0))$) is required for the u species to invade and colonize an empty patch in the absence of the v species. In that case, there is a unique positive solution $\tilde{w}_1$ of (2.2). Similarly, $\sigma_2 < 0$ (which will occur whenever $\lambda > E_1(r, h(0))$) is required for v, guaranteeing the existence of a unique positive solution $\tilde{w}_2$ of (2.3).

Next, we define two sets of principal eigenvalues that will be crucial to our main results. First, given a non-negative smooth function $a(x)$ defined on the patch Ω and define the principal eigenvalue $\sigma_3(a) = \sigma_3(\Omega, \lambda, r, a(x))$ with corresponding normalized eigenfunction $\phi_3 > 0;\ \overline{\Omega}$ of the following eigenvalue problem:

$$\begin{cases} -\Delta\phi - \lambda r\phi = \sigma\phi;\ \Omega \\ \frac{\partial\phi}{\partial\eta} + \sqrt{\lambda}h(a(x))\phi = \sigma\phi;\ \partial\Omega. \end{cases} \tag{2.6}$$

Denote $\overline{\sigma}_3(a) = \overline{\sigma}_3(\Omega, \lambda, r, a(x))$ and the corresponding normalized eigenfunction $\overline{\phi}_3 > 0;\ \overline{\Omega}$ of the eigenvalue problem that is the same as (2.6) but without the $\sigma\phi$ term on the boundary. For a fixed $\lambda > E_1(1, g(0))$, it is easy to see that when $\overline{\sigma}_3(\tilde{w}_1) > 0$, v will fail to invade the patch with u being established and near its steady–state, whereas $\overline{\sigma}_3(\tilde{w}_1) < 0$ will imply that v is able to invade the patch with u being already established (see [31]).

Second, given a non-negative smooth function $a(x)$, we define the principal eigenvalue $\sigma_4(a) = \sigma_4(\Omega, \lambda, a(x))$ with the corresponding normalized eigenfunction $\phi_4 > 0;\ \overline{\Omega}$ of the following eigenvalue problem:

$$\begin{cases} -\Delta\phi - \lambda\phi = \sigma\phi;\ \Omega \\ \frac{\partial\phi}{\partial\eta} + \sqrt{\lambda}g(a(x))\phi = \sigma\phi;\ \partial\Omega. \end{cases} \tag{2.7}$$

Denote $\overline{\sigma}_4(a) = \overline{\sigma}_4(\Omega, \lambda, a(x))$ and the corresponding normalized eigenfunction $\overline{\phi}_4 > 0;\ \overline{\Omega}$ of the eigenvalue problem that is the same as (2.7) but without the $\sigma\phi$ term on the boundary. For a fixed $\lambda > E_1(r, h(0))$, it is easy to see that when $\overline{\sigma}_4(\tilde{w}_2) > 0$, u will fail to invade the patch with v being established and near its steady–state, whereas $\overline{\sigma}_4(\tilde{w}_2) < 0$ will imply that u is able to invade the patch with v being already established. We note that Lemma 5 on page 15 of [31] establishes $sgn(\sigma_i) = sgn(\overline{\sigma}_i),\ i = 3, 4$.

The following lemma will aid us in determining the sign of these σ_i principal eigenvalues.

Lemma 2.1 ([31, 32])**.** *Let $\mu_1 = \mu_1(\beta)$ denote the principal eigencurve associated with the following linear boundary value problem:*

$$\begin{cases} -\Delta\phi = \mu\phi;\ \Omega \\ \frac{\partial\phi}{\partial\eta} + \beta(x)\phi = 0;\ \partial\Omega, \end{cases} \tag{2.8}$$

where β is a non-negative continuous function on $\partial\Omega$. Then μ_1 increases in β (see [32]). For a fixed $\gamma > 0$, when $\beta = \sqrt{\lambda}\gamma$, by Lemmas 2 and 3 in [31], the principal eigencurve $\mu_1(\sqrt{\lambda}\gamma)$ is strictly

increasing and concave in λ. *Moreover,* $\mu_1(0) = 0$ *and* $\mu_1(\sqrt{\lambda}\gamma) \to E_1^D$ *as* $\lambda \to \infty$, *where* E_1^D *is the principal eigenvalue of*

$$\begin{cases} -\Delta\phi = E\phi; \ \Omega \\ \phi = 0; \ \partial\Omega, \end{cases}$$

with the corresponding eigenfunction $\phi(x) > 0; \ \overline{\Omega}$, *which is a special case of* (2.1).

Comparing (2.4)–(2.7) with (2.8) in Lemma 2.1, we obtain explicit expressions for σ_1, σ_2, $\overline{\sigma}_3$, and $\overline{\sigma}_4$ so that we can determine their sign for ranges of λ as follows:

$$\sigma_1 = \mu_1(\sqrt{\lambda}g(0)) - \lambda, \tag{2.9}$$

$$\sigma_2 = \mu_1(\sqrt{\lambda}h(0)) - \lambda r, \tag{2.10}$$

$$\overline{\sigma}_3(a) = \mu_1(\sqrt{\lambda}h(a)) - \lambda r, \tag{2.11}$$

$$\overline{\sigma}_4(a) = \mu_1(\sqrt{\lambda}g(a)) - \lambda. \tag{2.12}$$

2.2. Case 1: Trait–mediated competition ($g \uparrow, h \uparrow$*)*

Here, we extend the results of [22] by examining trait–mediated competition between two species. In (1.3), this assumption is integrated by assuming that g, h are increasing functions of competitor density. Ecologically, this means density-dependent emigration for u increases when the density of v increases and vice versa. In the literature, this is referred to as +DDE. As we established in Section 2.1, the minimum patch size (MPS) for the species u (v) to colonize an empty patch is related to $E_1(1, g(0))$ ($E_1(r, h(0))$). Thus, for any fixed $g(0), h(0) > 0$, by continuity and monotonicity in the first argument of E_1, an $r^* > 0$ (see Lemma 2.1 in [22]) exists such that $E_1(1, g(0)) = E_1(r^*, h(0))$. Then, depending on the assumed order of $g(0)$ and $h(0)$ and that of r with respect to r^*, the order of $E_1(1, g(0))$ relative to $E_1(r, h(0))$ is determined. This is important in establishing the signs of related eigenvalues (variations of the problems associated with ϕ_3, ϕ_4 above) for ranges of λ, for which our nonexistence and coexistence results depend (see the eigencurve analysis as shown in [22]).

Table 1. Relationship between the critical ratio r^* and the principal eigenvalues.

Assumption	Result
$g(0) < h(0)$	$r^* > 1$
$g(0) > h(0)$	$r^* < 1$
$g(0) = h(0)$	$r^* = 1$

Assumption	Eigenvalues ordering	Meaning
$r < r^*$	$E_1(1, g(0)) < E_1(r, h(0))$	u has smaller MPS
$r > r^*$	$E_1(1, g(0)) > E_1(r, h(0))$	v has smaller MPS
$r = r^*$	$E_1(1, g(0)) = E_1(r, h(0))$	u and v have same MPS

Defining

$$\lambda^{1,1} = \max\{E_1(1, g(1)), E_1(r, h(1))\}$$

$$\lambda^{0,0} = \max\{E_1(1, g(0)), E_1(r, h(0))\},$$

we state our main results in Theorems 2.1–2.3.

Theorem 2.1. *Given $r > 0$, we have the following:*

(a) For $\lambda \le \lambda^{0,0}$, (1.3) has no positive solution.

(b) For $\lambda > \lambda^{1,1}$, (1.3) has a positive solution (u, v).

(c) If (1.3) has a positive solution (u, v) for $\lambda > \lambda^{0,0}$, then we must have

$$\begin{aligned} 0 < u < \tilde{w}_1;\ \overline{\Omega} \\ 0 < v < \tilde{w}_2;\ \overline{\Omega} \end{aligned} \tag{2.13}$$

where $\tilde{w}_1(x)$ and $\tilde{w}_2(x)$ are the unique positive solutions of (2.2) and (2.3), respectively.

Theorem 2.2. *Let $r \in (0, r^*)$, implying that $E_1(1, g(0)) < E_1(r, h(0))$ (u has a smaller MPS requirement when alone). Then a $\xi_1 > 0$ exists such that (1.3) has no positive solution for $\lambda < E_1(r, h(0)) + \xi_1$.*

Theorem 2.3. *Let $r > r^*$, implying that $E_1(r, h(0)) < E_1(1, g(0))$ (v has a smaller MPS requirement when alone). Then a $\xi_2 > 0$ exists such that (1.3) has no positive solution for $\lambda < E_1(1, g(0)) + \xi_2$.*

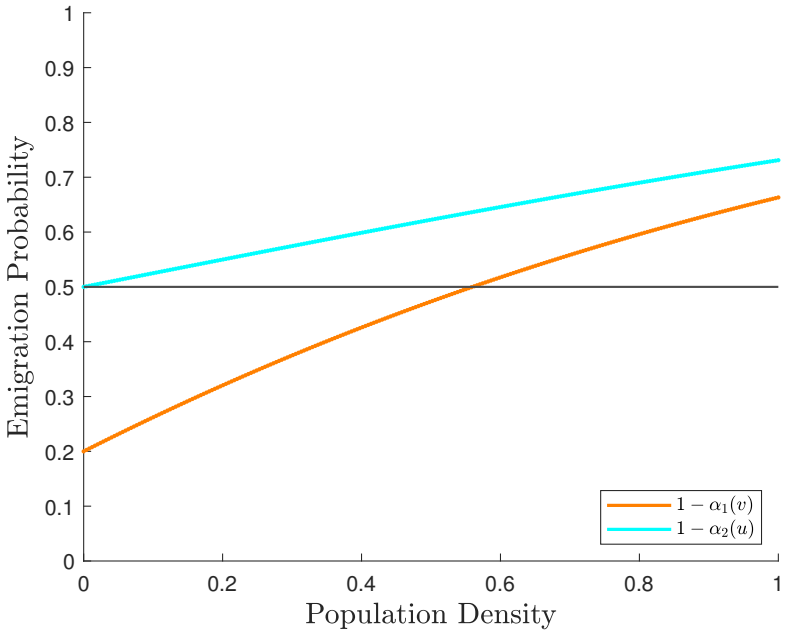

Figure 1. Emigration form for u, given as $1 - \alpha_1(v) = \frac{-3+4\exp(v)}{1+4\exp(v)}$ (in orange), and for v, given as $1 - \alpha_2(u) = \frac{\exp(u)}{1+\exp(u)}$ (in cyan).

Theorem 2.1 illustrates three ideas: (1) Coexistence is not possible for patches that are too small, i.e., for patches with $\lambda \in \left(0, \lambda^{0,0}\right]$, (2) coexistence is guaranteed for patches that are significantly large, i.e., patches with $\lambda \in (\lambda^{1,1}, \infty)$, and (3) whenever coexistence occurs, the coexistence state will always

be smaller than the density of the organisms in the patch without their competitor. Theorems 2.2 and 2.3 show that even though both competitors are able to invade and colonize an empty patch for patch sizes with $\lambda > \lambda^{0,0}$, trait–mediated competitive exclusion prohibits their coexistence for patch sizes with $\lambda \in \left[\lambda^{0,0}, \lambda^{0,0} + \xi\right)$ for some $\xi > 0$. It is interesting to note that this is in contrast to the cooperative case (g, h are decreasing functions of competitor density), where coexistence was shown to occur at patch sizes corresponding to values of λ between $E_1(1, g(0))$ and $E_1(r, h(0))$ (see Figure 8 in [22]).

We also computationally produced bifurcation diagrams for positive solutions of (1.3) for the case of the one-dimensional patch, $\Omega = (0, 1)$, using the quadrature method (see Section 3.2 for implementation details) for several choices of g, h where we observed interesting model predictions. The first example assumes the emigration forms $1 - \alpha_1(v) = \frac{-3+4\exp(v)}{1+4\exp(v)}$ for u and $1 - \alpha_2(u) = \frac{\exp(u)}{1+\exp(u)}$ for v and $r = 1$, which implies that $E_1(1, g(0)) < E_1(r, h(0))$ (see Figure 1). We note that the emigration probability for v dominates the emigration probability for u, with the effect being more pronounced for v, relative to u (see Figure 1). Figure 2 shows the numerical bifurcation diagram of positive solutions for (1.3) that we produced, and Figure 3 gives biological meaning to the various λ-ranges outlined in Theorems 2.1–2.3.

The second example assumes the emigration forms $1 - \alpha_1(v) = \frac{1+v}{2+v}$ for u and $1 - \alpha_2(u) = \frac{1+2u}{2(1+u)}$ for v and $r = 2$, which implies that $E_1(1, g(0)) > E_1(r, h(0))$ (see Figure 4). Figure 5 shows the numerical bifurcation diagram of positive solutions for (1.3) that we produced, and Figure 6 gives biological meaning to the various λ-ranges outlined in Theorems 2.1–2.3.

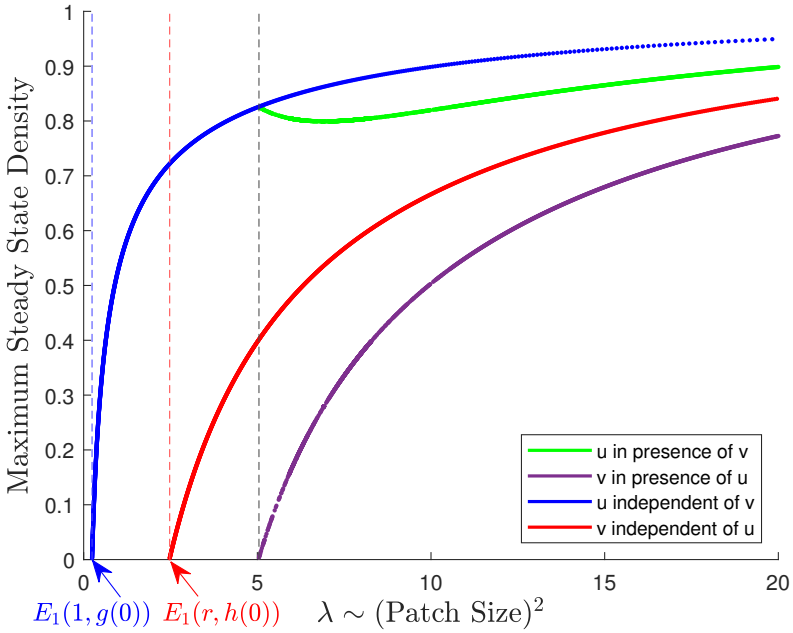

Figure 2. Bifurcation diagram of positive solutions of (1.3) for the case when $\Omega = (0, 1)$, $g(v) = -\frac{3}{4} + \exp(v), h(u) = \exp(u)$, and $r = 1$, where, for these choices, $E_1(1, g(0)) < E_1(r, h(0))$.

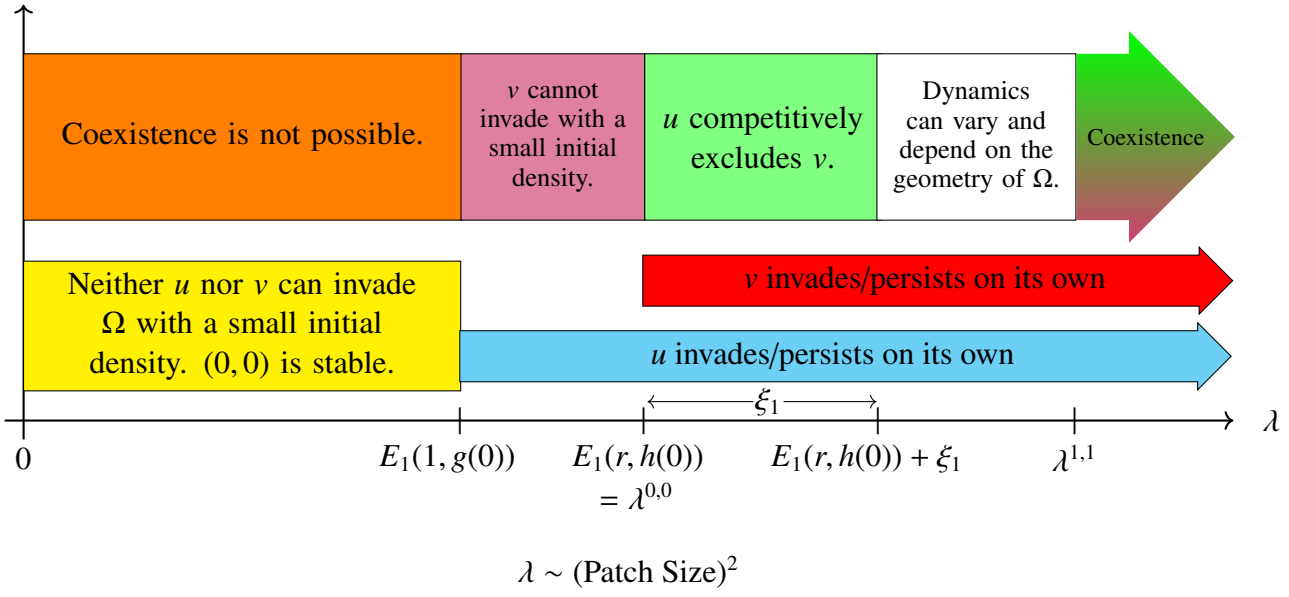

Figure 3. Model predictions over λ (patch size squared) based on Theorems 2.1–2.3 in the case when $E_1(1, g(0)) < E_1(r, h(0))$.

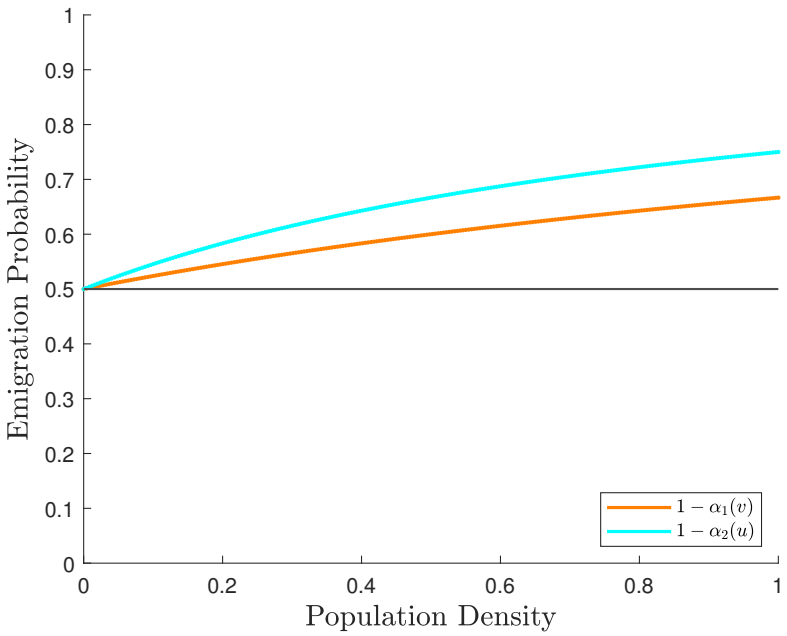

Figure 4. Emigration form for u, given as $1 - \alpha_1(v) = \frac{1+v}{2+v}$ (in orange), and for v, given as $1 - \alpha_2(u) = \frac{1+2u}{2(1+u)}$ (in cyan).

The third example assumes the emigration forms $1 - \alpha_1(v) = \frac{41+2500v^2}{441+2500v^2}$ for u, $1 - \alpha_2(u) = \frac{3+25u^2}{4+25u^2}$ for v, and $r = 1.25$, which implies that $E_1(1, g(0)) < E_1(r, h(0))$ (see Figure 7). Figure 8 shows the numerical bifurcation diagram of positive solutions for (1.3) that we produced. For this case, we used the function `NDEigenSystem` in Wolfram Mathematica (Wolfram Research Inc., version 13.0)

to numerically estimate the principal eigenvalues $\sigma_i; i = 3, 4$ over λ. The single–species steady–state solutions, $\tilde{w}_1$ and $\tilde{w}_2$, were numerically estimated using the quadrature method outlined in Section 3.2. Figure 9 gives biological meaning to the various λ-ranges observed from our computational estimates of the principal eigenvalues $\sigma_i; i = 3, 4$.

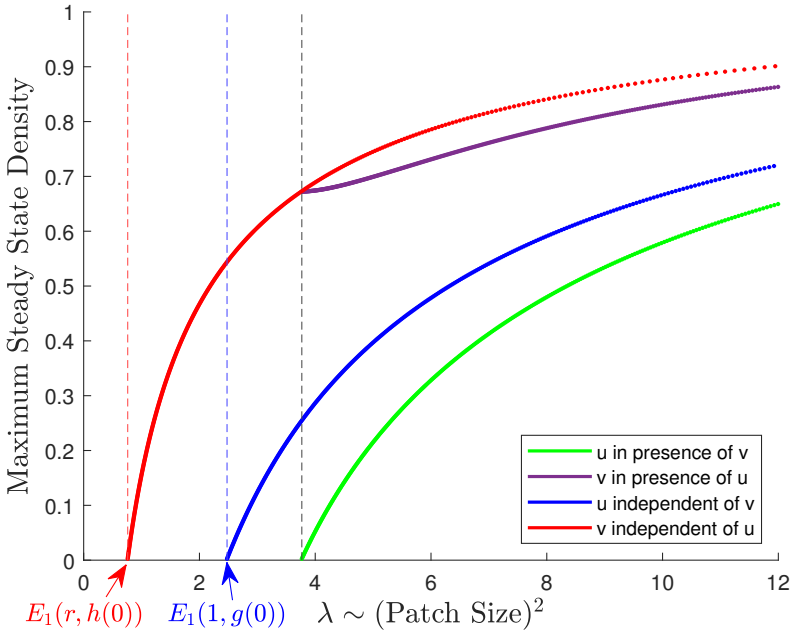

Figure 5. Bifurcation diagram of positive solutions of (1.3) for the case when $\Omega = (0, 1)$, $g(v) = 1 + v, h(u) = 1 + 2u,$ and $r = 2$, where, for these choices, $E_1(1, g(0)) > E_1(r, h(0))$.

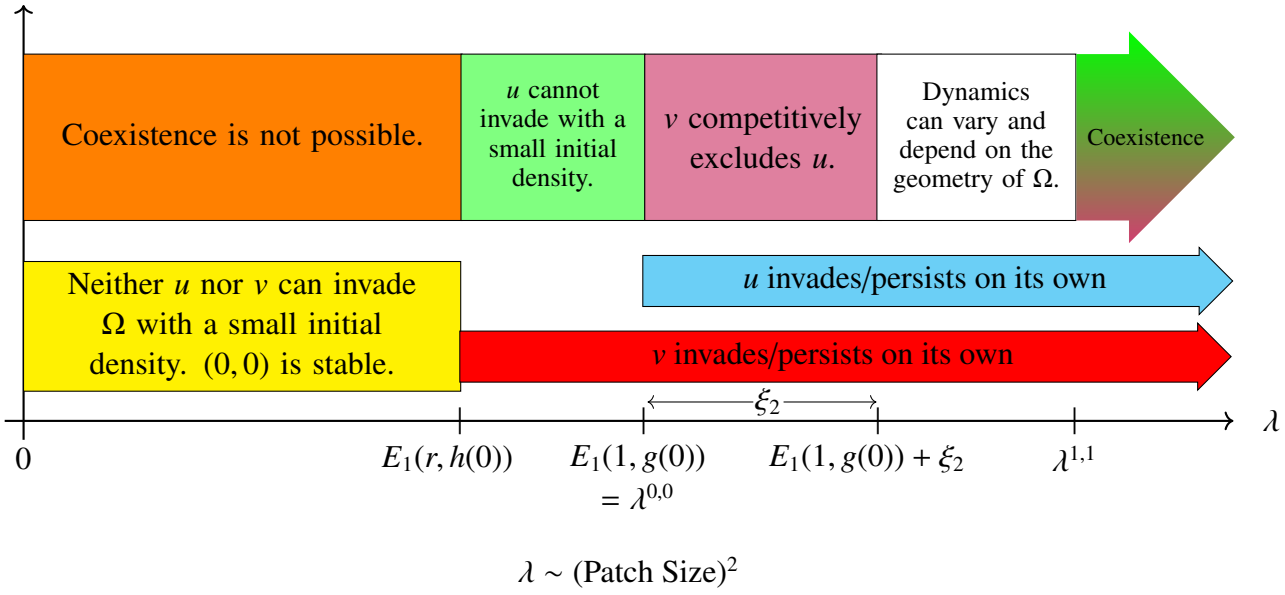

Figure 6. Model predictions over λ (patch size squared) based on Theorems 2.1–2.3 in the case when $E_1(r, h(0)) < E_1(1, g(0))$.

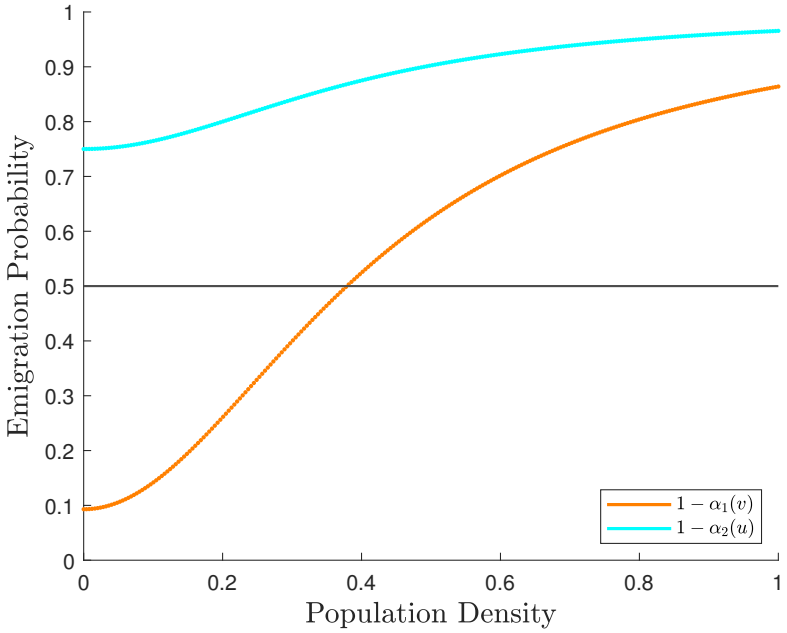

Figure 7. Emigration form for u, given as $1-\alpha_1(v) = \frac{41+2500v^2}{441+2500v^2}$ (in orange), and for v, given as $1-\alpha_2(u) = \frac{3+25u^2}{4+25u^2}$ (in cyan).

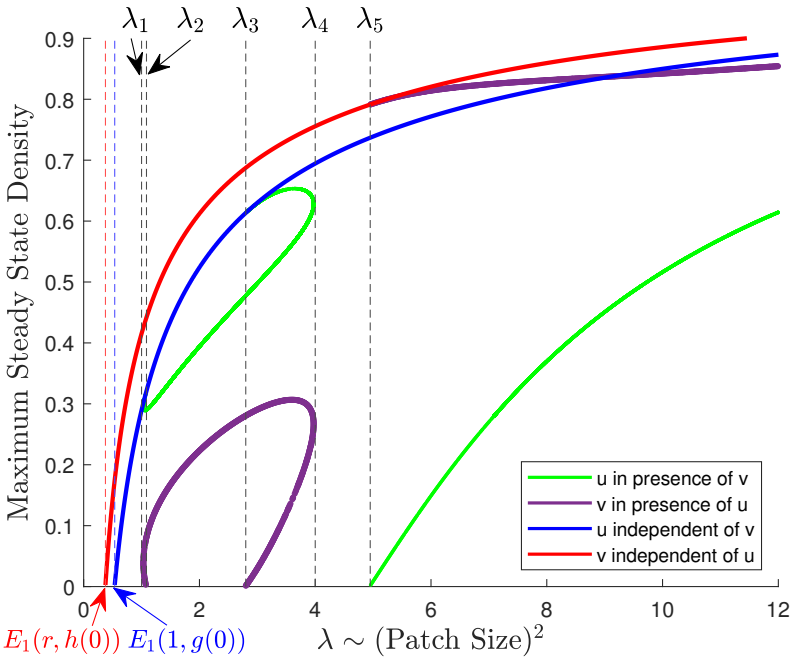

Figure 8. Bifurcation diagram of positive solutions of (1.3) for the case when $\Omega = (0,1)$, $g(v) = \frac{25}{4}v^2 + \frac{41}{100}$, $h(u) = 25u^2 + 3$, and $r = 1.25$, where, for these choices, $E_1(r,h(0)) < E_1(1,g(0))$.

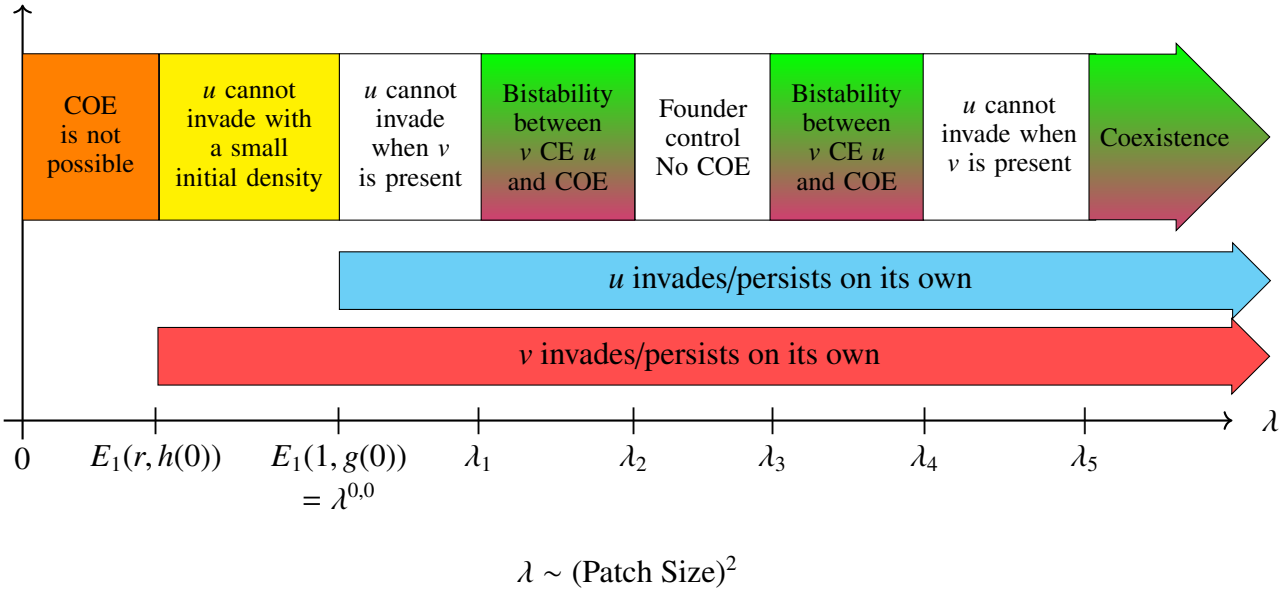

Figure 9. Existence versus λ when $E_1(r, h(0)) < E_1(1, g(0))$. Note that CE represents competitive exclusion of the competitor and COE represents coexistence between the competitors.

2.2.1. Biological interpretation

In all three examples, we observe the conclusions of our main results given in Theorems 2.1–2.3, i.e., for patches whose size is too small, coexistence is not possible, and for sufficiently large patch sizes, coexistence is always predicted. When the patch size is sufficiently large, a core patch area develops allowing both species to coexist even under the pressure of high emigration rates and increased mortality due to encountering the hostile matrix. This occurs whenever the patch becomes large enough relative to the patch diffusion rate that a significant proportion of the population remains away from the patch–matrix interface, and thus avoids mortality due to the hostile matrix (see, e.g., [17] for a detailed discussion of core patch area in the context of reaction diffusion models). As Theorem 2.1 predicted, we observe that the coexistence states (green for u and purple for v) in Figures 2, 5, and 8 have a lower maximum steady–state density than the competitor-independent states (blue for u and red for v). This phenomenon is due to the increased emigration and mortality experienced in the hostile matrix caused by higher competitor density in the patch. In the first two examples, whichever species had the smaller minimum patch size requirement, as measured by the E_1 principal eigenvalue, had a competitive advantage in that they were able to invade and colonize smaller patches than their competitor (see Figures 3 and 6). Moreover, for patches with $\lambda > \lambda^{0,0}$ and $\lambda \approx \lambda^{0,0}$, the organism with the smaller minimum patch size is predicted to competitively exclude its competitor. Since the direct effects of competition are not included in the model, this competitive exclusion is due solely to trait–mediated competition. In this case when the patch size has $\lambda \approx \lambda^{0,0}$, the competitor's density is large enough relative to the +DDE strength that excessively high trait–mediated emigration and mortality in the hostile matrix overcomes the organism's reproductive ability.

The third example shows that a wide range of interesting biological phenomena are possible with trait–mediated competition. First, we see a range of intermediate patch sizes corresponding to $\lambda \in$

(λ_2, λ_3), where a priority effect (which is also known as founder control in the literature) is predicted by the model. In this case, whichever competitor is able to colonize the patch first will repel invasion from the other competitor. The dynamic mechanism observed in these numerical results (i.e., both semi–trivial states being stable and the existence of an unstable coexistence state) is functionally similar to the mechanism behind the priority effects in the spatially homogeneous Lotka–Volterra competition model for sufficiently high competitive coefficients. For patch sizes corresponding to $\lambda \in (\lambda_1, \lambda_2) \cup (\lambda_3, \lambda_4)$, there is a novel bistability between a coexistence state and the semi–trivial state $(0, v)$ (which implies that v competitively excludes u via trait–mediated dispersal) that is predicted by the model. In other words, if v is able to colonize the patch near its single–species steady–state density, then it is able to resist invasion by its competitor u. However, if u colonizes the patch first, then an invasion by v will be successful and lead to coexistence between the species, albeit with u having a much larger maximum steady–state density than v. For patch sizes corresponding to $\lambda \in (\lambda^{0,0}, \lambda_1) \cup (\lambda_4, \lambda_5)$, we observe what we call a "dead zone", where both species are able to colonize the patch when alone, but v will competitively exclude u. Similar dead zone effects have been observed in [23] but in a different context. We note that since our model assumes that direct competitive effects are negligible, these effects are due solely to trait–mediated emigration. From a mechanistic perspective, trait–mediated emigration causes each competitor to increase its emigration probability as a function of competitor density, which, in turn, causes more of the population to emigrate into the hostile matrix and experience mortality there.

2.3. Case 2: Non–consumptive predator–prey $(g \uparrow, h \downarrow)$

Here, we continue extension of the results in [22] and [23] by examining trait–mediated effects in a non–consumptive predator–prey setting. In (1.3), this assumption is again integrated by assuming that g is increasing as a function of predator density and h is decreasing as a function of prey density. Ecologically, this means that density-dependent emigration for u (prey) increases when the density of v (predator) increases (+DDE) and density-dependent emigration for v (predator) decreases when the density of u (prey) increases (-DDE). As in the previous subsection, the ordering of the principal eigenvalues $E_1(1, g(0))$ and $E_1(r, h(0))$ will play an important role in our results.

In addition to $\lambda^{1,1}$ and $\lambda^{0,0}$ defined in Case 1, we define

$$\begin{aligned}\lambda^{1,0} &= \max\{E_1(1, g(1)), E_1(r, h(0))\}\\ \lambda^{0,1} &= \max\{E_1(1, g(0)), E_1(r, h(1))\}.\end{aligned}$$

Our results also crucially depend upon a counterpart to the semi–trivial steady–states where it is assumed the patch is devoid of one species, i.e., $\tilde{w}_i;\ i = 1, 2$. In this case, we consider the other extreme by assuming (for the prey) that the predator is uniformly distributed in the patch at 100% of the carrying capacity, namely w_1^*, and (for the predator) that the prey is uniformly distributed in the patch at 100% of the carrying capacity, namely w_2^*. For $\lambda > E_1(1, g(1))$, we denote w_1^* as the unique positive solution to

$$\begin{cases} -\Delta w = \lambda w(1 - w);\ \Omega \\ \frac{\partial w}{\partial \eta} + \sqrt{\lambda} g(1) w = 0;\ \partial\Omega \end{cases} \tag{2.14}$$

and for $\lambda > E_1(r, h(1))$, we denote w_2^* as the unique positive solution to

$$\begin{cases} -\Delta w = \lambda r w(1-w); \ \Omega \\ \frac{\partial w}{\partial \eta} + \sqrt{\lambda} h(1) w = 0; \ \partial\Omega. \end{cases} \tag{2.15}$$

We are now ready to state our main results in Theorems 2.4–2.6.

Theorem 2.4. *Given $r > 0$, we have the following:*

(a) For $\lambda \le \lambda^{0,1}$, (1.3) has no positive solution.

(b) For $\lambda > \lambda^{1,0}$, (1.3) has a positive solution (u, v).

(c) If (1.3) has a positive solution (u, v) for $\lambda > \lambda^{0,1}$, then we must have

$$\begin{aligned} 0 < u < \tilde{w}_1 < 1; \ \overline{\Omega} \\ 0 < v < w_2^* < 1; \ \overline{\Omega} \end{aligned} \tag{2.16}$$

where $\tilde{w}_1$ and w_2^* are the unique positive solutions of (2.2) and (2.15), respectively. Moreover, if we additionally assume that $\lambda > E_1(r, h(0))$, then we also have

$$0 < \tilde{w}_2 < v < w_2^* < 1; \ \overline{\Omega}$$

where $\tilde{w}_2$ is the unique positive solution of (2.3).

Theorem 2.5. *Let $r < r^*$, implying that $E_1(1, g(0)) < E_1(r, h(0))$ (the prey u has a smaller MPS requirement when alone). Then we have*

(a) If $\lambda^{0,1} = E_1(r, h(1))$ and $\lambda^{1,0} = E_1(1, g(1))$, then $\xi_1 > 0$ exists such that (1.3) has no positive solution for $\lambda < \lambda^{0,1} + \xi_1$.

(b) If $\lambda^{0,1} = E_1(r, h(1))$ and $\lambda^{1,0} = E_1(r, h(0))$, then $\xi_2, \delta_2 > 0$ exist such that (1.3) has no positive solution for $\lambda < \lambda^{0,1} + \xi_2$ and has a positive solution (u, v) for $\lambda > \lambda^{1,0} - \delta_2$.

(c) If $\lambda^{0,1} = E_1(1, g(0))$ and $\lambda^{1,0} = E_1(1, g(1))$, then $\xi_3 > 0$ exists such that (1.3) has no positive solution for $\lambda < \lambda^{0,1} + \xi_3$.

(d) If $\lambda^{0,1} = E_1(1, g(0))$ and $\lambda^{1,0} = E_1(r, h(0))$, then$\xi_4, \delta_4 > 0$ exist such that (1.3) has no positive solution for $\lambda < \lambda^{0,1} + \xi_4$ and has a positive solution (u, v) for $\lambda > \lambda^{1,0} - \delta_4$.

Theorem 2.6. *If $r > r^*$, implying that $E_1(r, h(0)) < E_1(1, g(0))$ (the prey u has a larger MPS requirement when alone), then $\lambda^{0,1} = E_1(1, g(0))$, $\lambda^{1,0} = E_1(1, g(1))$, and $\xi_5 > 0$ exists such that (1.3) has no positive solution for $\lambda < \lambda^{0,1} + \xi_5$.*

Theorem 2.4 illustrates three ideas: (1) coexistence is not possible for patches that are too small, i.e., for patches with $\lambda \in \left(0, \lambda^{0,0}\right]$; (2) coexistence is guaranteed for patches that are significantly large, i.e., patches with $\lambda \in (\lambda^{1,0}, \infty)$; and (3) whenever coexistence occurs, the prey component's density will be smaller and the predator's density will be greater than their corresponding semi–trivial steady–state density. Theorem 2.5 explores the case where the prey has a smaller MPS requirement allowing it to occupy much smaller patches than its predator. The two main predictions of the result are (1)

under certain conditions related to the DDE strength of both species, the predator is able to invade and colonize a patch where the prey is already established near its carrying capacity even though the predator would fail to colonize the same size patch in the absence of prey, which is a form of a facilitation effect, and (2) this facilitation effect is not possible for patches with $\lambda \approx E_1(r, h(0))$, where the prey density would be too small to aid in the predator's colonization attempt. Theorem 2.6 combined with Theorem 2.4 shows that this facilitation effect is not possible when the predator has the smaller MPS requirement.

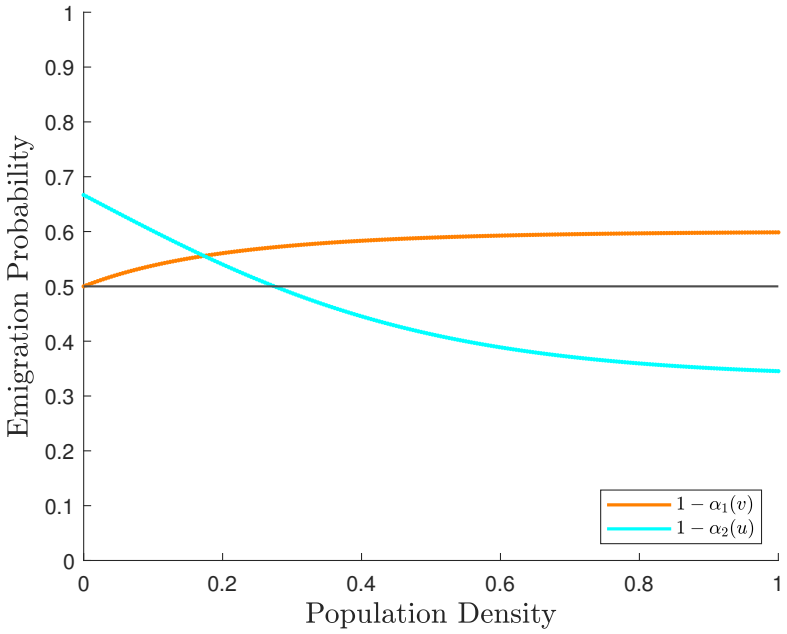

Figure 10. Emigration form for u, given as $1-\alpha_1(v) = \frac{3-\exp(-4v)}{5-\exp(-4v)}$ (in orange), and for v, given as $1-\alpha_2(u) = \frac{1+3\exp(-4u)}{3(1+\exp(-4u))}$ (in cyan).

We also computationally produced bifurcation diagrams for positive solutions of (1.3) for the case of the one-dimensional patch, $\Omega = (0, 1)$, using the quadrature method (see Section 3.2) for several choices of g, h where we observed interesting model predictions. The first example assumes the emigration forms $1-\alpha_1(v) = \frac{3-\exp(-4v)}{5-\exp(-4v)}$ for u and $1-\alpha_2(u) = \frac{1+3\exp(-4u)}{3(1+\exp(-4u))}$ for v with $r = 1$, which implies that $E_1(1, g(0)) < E_1(r, h(0))$, and Case (d) from Theorem 2.5 applies (see Figure 10). We note that the emigration probability for v initially dominates the emigration probability for u but this is quickly reversed as the other organism's density increases (see Figure 10). Figure 11 shows the numerical bifurcation diagram of positive solutions for (1.3) that we produced, and Figure 12 gives biological meaning to the various λ-ranges outlined in Theorems 2.4–2.6.

The second example assumes the emigration forms $1-\alpha_1(v) = \frac{2+\exp(5v)}{3+\exp(5v)}$ for u and $1-\alpha_2(u) = \frac{2\exp(-5u)}{1+2\exp(-5u)}$ for v with $r = 1$, which implies that $E_1(r, h(0)) < E_1(1, g(0))$ and Theorem 2.6 applies (see Figure 13). We note that the emigration probability for u dominates the emigration probability for v (see Figure 13). Figure 14 shows the numerical bifurcation diagram of positive solutions for (1.3) that we produced, and Figure 15 gives biological meaning to the various λ-ranges outlined in Theorems 2.4–2.6.

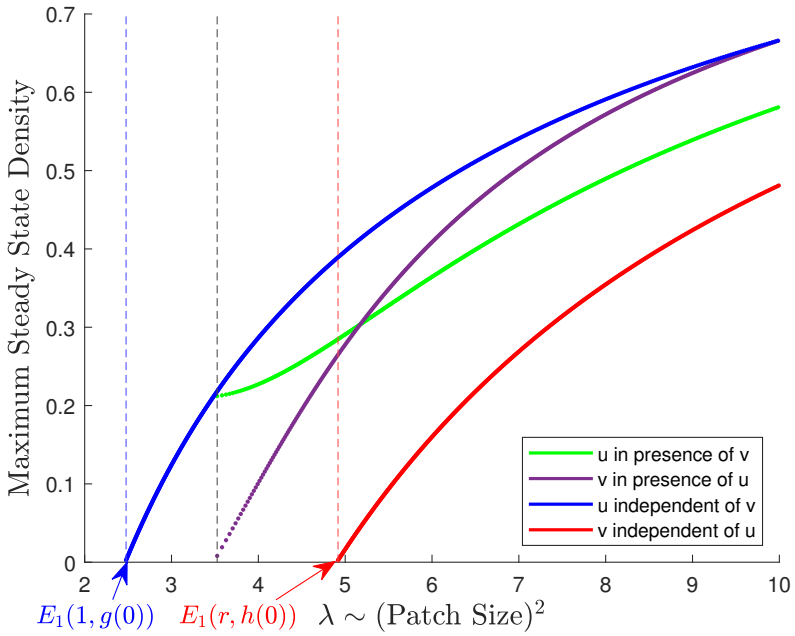

Figure 11. Bifurcation diagram of positive solutions of (1.3) for the case when $\Omega = (0, 1)$, $g(v) = \frac{3}{2} - \frac{1}{2}\exp(-4v)$, $h(u) = \frac{1}{2} + \frac{3}{2}\exp(-4u)$, and $r = 1$, where, for these choices, $E_1(1, g(0)) < E_1(r, h(0))$.

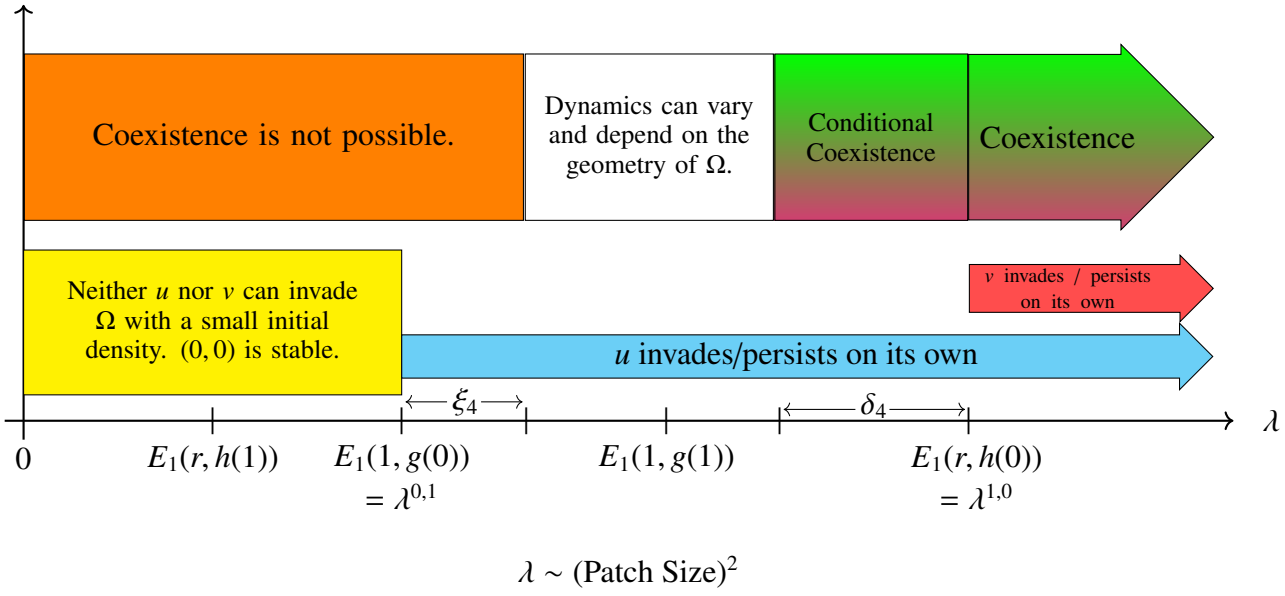

Figure 12. Existence versus λ when $E_1(1, g(0)) < E_1(1, g(1)) < E_1(r, h(0)) - \delta_4$.

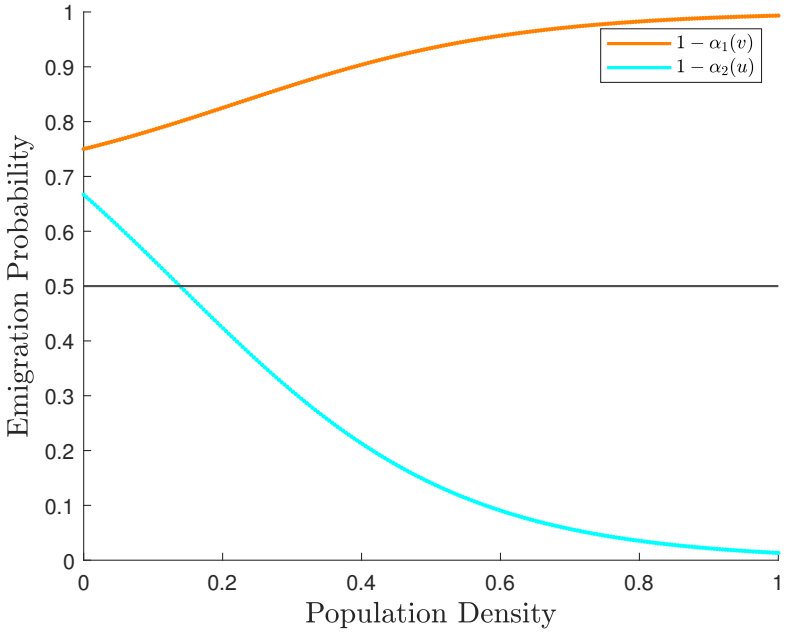

Figure 13. Emigration form for u, given as $1-\alpha_1(v) = \frac{2+\exp(5v)}{3+\exp(5v)}$ (in orange), and for v, given as $1-\alpha_2(u) = \frac{2\exp(-5u)}{1+2\exp(-5u)}$ (in cyan).

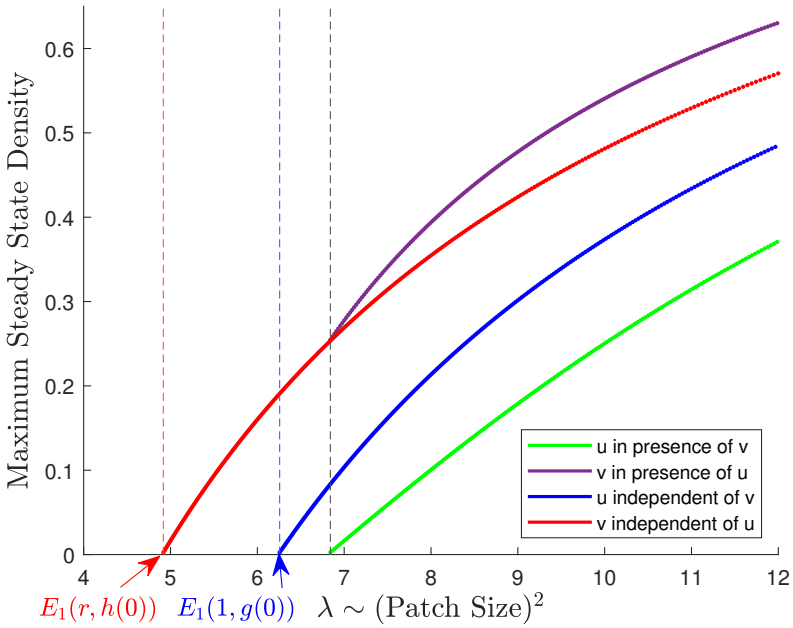

Figure 14. Bifurcation diagram of positive solutions of (1.3) for the case when $\Omega = (0,1)$, $g(v) = 2+\exp(5v)$, $h(u) = 2\exp(-5u)$, and $r = 1$, where, for these choices, $E_1(r,h(0)) < E_1(1,g(0))$.

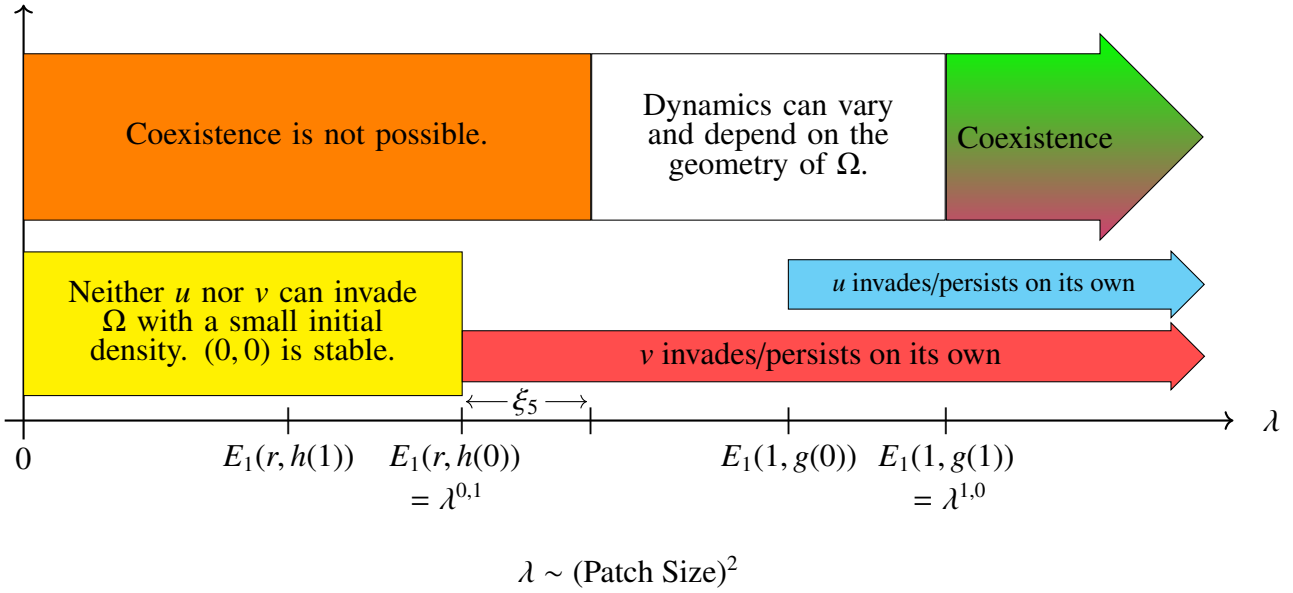

Figure 15. Existence versus λ when $E_1(r, h(0)) < E_1(1, g(0))$.

The final two examples illustrate some interesting phenomena that are not predicted by our main results. The third example assumes the emigration forms $1 - \alpha_1(v) = \frac{\exp(v)}{1+\exp(v)}$ for u and $1 - \alpha_2(u) = \frac{\exp(-u)}{1+\exp(-u)}$ for v with $r = 1$, which implies that $E_1(r, h(0)) = E_1(1, g(0))$ (see Figure 13). We note that the emigration probabilities for both begin at 50% and have equal but opposite slopes (see Figure 16). Figure 17 shows the numerical bifurcation diagram of positive solutions for (1.3) that we produced.

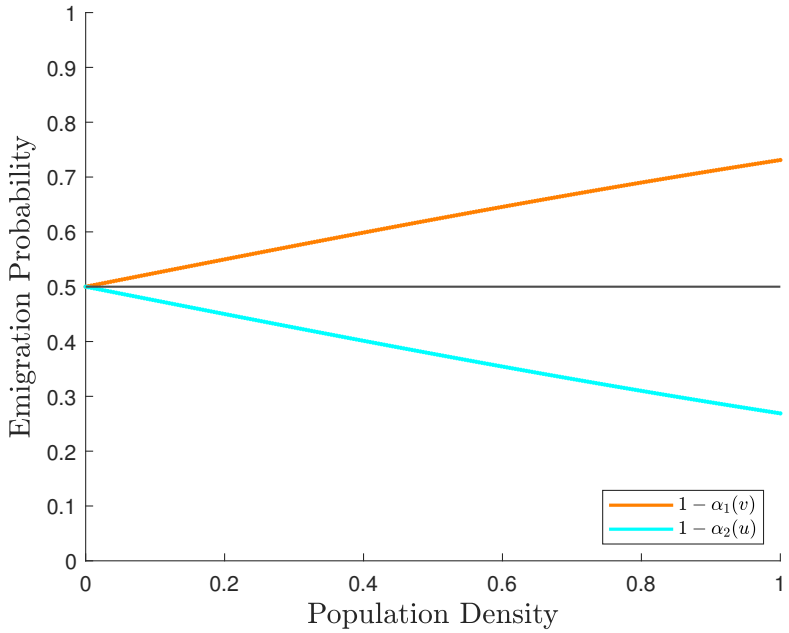

Figure 16. Emigration form for u, given as $1 - \alpha_1(v) = \frac{\exp(v)}{1+\exp(v)}$ (in orange), and for v, given as $1 - \alpha_2(u) = \frac{\exp(-u)}{1+\exp(-u)}$ (in cyan).

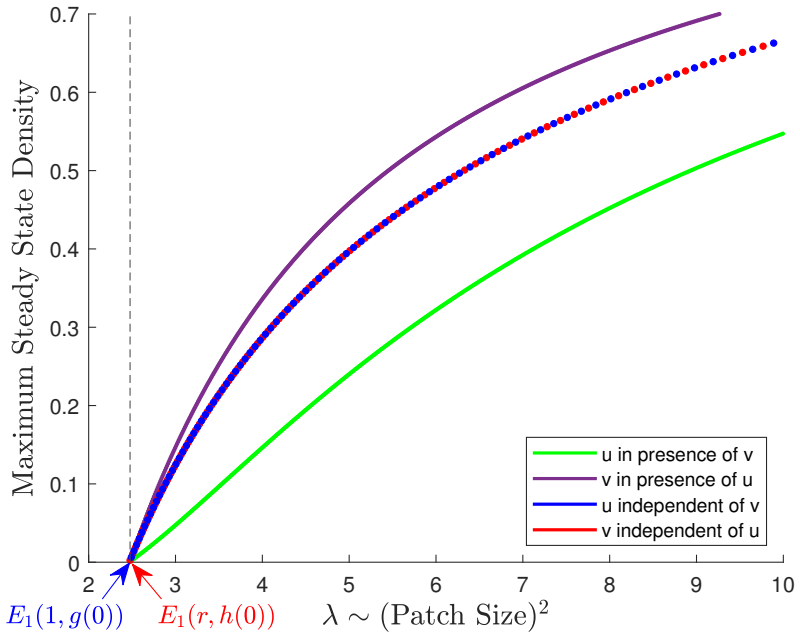

Figure 17. Bifurcation diagram of positive solutions for (1.3) in the case when $\Omega = (0, 1)$, $g(v) = \exp(v), h(u) = \exp(-u)$, and $r = 1$, where, for these choices, we have $E_1(r, h(0)) = E_1(1, g(0))$.

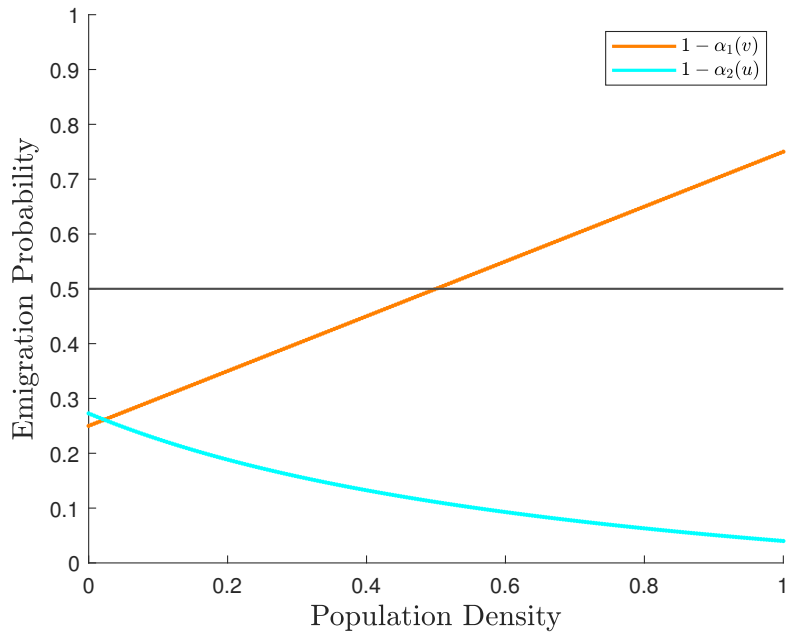

Figure 18. Emigration form for u, given as $1 - \alpha_1(v) = \frac{1}{4} + \frac{1}{2}v$ (in orange), and for v, given as $1 - \alpha_2(u) = \frac{3-2u}{11+14u}$ (in cyan).

The final example assumes the emigration forms $1-\alpha_1(v) = \frac{1}{4} + \frac{1}{2}v$ for u and $1-\alpha_2(u) = \frac{3-2u}{11+14u}$ for v

with $r = 1$, which implies that $E_1(r, h(0)) < E_1(1, g(0))$ (see Figure 18). Figure 19 shows the numerical bifurcation diagram of positive solutions for (1.3) that we produced.

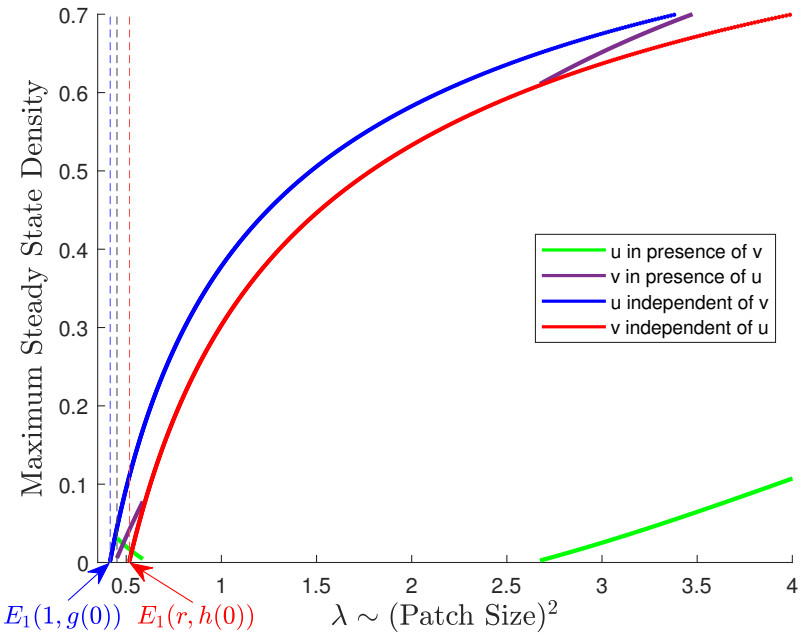

Figure 19. Bifurcation diagram of positive solutions for (1.3) in the case when $\Omega = (0, 1)$, $g(v) = \frac{1+2v}{3-2v}$, $h(u) = \frac{1}{8}\left(\frac{3-2u}{1+2u}\right)$, and $r = 1$, where, for these choices, we have $E_1(1, g(0)) < E_1(r, h(0))$.

2.3.1. Biological interpretation

In all four examples, we observe the conclusions of our main results given in Theorems 2.4–2.6. For patches whose size is too small, persistence is not possible, while for sufficiently large patch sizes, coexistence is always predicted. When the patch size is sufficiently large, a core patch area develops allowing both species to coexist even under the stress of high prey emigration rates and increased mortality due to encountering the hostile matrix (see, e.g., [17] for a detailed discussion of the core patch area in the context of reaction diffusion models). As Theorem 2.4 predicted, we observe that the coexistence states (green for u and purple for v) in Figures 11, 14, 17, and 19 show that the prey u have a lower and the predators have a higher maximum steady–state density than the independent states (blue for u and red for v). This phenomenon is due, in the prey, to the increased emigration and mortality experienced in the hostile matrix caused by higher predator density in the patch, and, for the predator, is caused by the decreased emigration and mortality experienced in the matrix due to higher prey density.

In certain cases where prey has a smaller MPS requirement (see Figures 11 and 12), a facilitation effect (i.e., a positive unidirectional interaction where the predator benefits from the presence of the prey), occurs for a range of patch sizes corresponding to $\lambda \in [E_1(r, h(0)) - \delta, E_1(r, h(0))]$ for some $\delta > 0$. In this case, if the prey are already established and near their steady–state, the -DDE of the predator lowers losses due to encountering the hostile matrix to the point that the predator is able to successfully invade and colonize a patch which, without the prey being present, they would not be able to colonize.

We note that since the model does not feature direct predator–prey effects, this facilitation effect is due directly to trait–mediated dispersal. This effect also makes the predator intricately dependent upon its prey for this range of patch sizes. In other words, if, for a patch in the facilitation effect range, the prey is eliminated from the patch, then the predator population would be predicted to go extinct in the patch and be unable to recolonize the patch until the prey species is reintroduced and has returned to near steady–state levels.

In cases where the predator has a smaller MPS requirement, the prediction of predator-mediated exclusion of the prey listed in Theorem 2.6 can be observed in Figures 14 and 15 for patch sizes with a corresponding $\lambda \in [E_1(r, h(0)), E_1(r, h(0)) + \xi]$ (for some $\xi > 0$). Again, since there are no direct predation effects in the model, this is an example of trait–mediated exclusion arising from the increased prey emigration rates leading to the prey encountering higher mortality from the hostile matrix. Mechanistically, in patches with size larger than but close to the prey's MPS requirement in the absence of predators, the increased emigration due to the presence of the predator overcome the prey's reproductive ability, leading to a prediction of extinction in a patch that the prey could colonize in the absence of their predator. In other words, prey established in a patch in this range without their predator present would be predicted to go extinct if their predator were to invade and colonize the patch.

Figures 16 and 17 show a case where the prey and predator have the same MPS requirement. Here, coexistence is predicted for any patch with a size larger than this MPS requirement. We observe neither facilitation nor trait–mediated exclusion in this case. Finally, Figures 18 and 19 show a scenario where the predator has a slightly smaller MPS requirement than its prey. In this case, coexistence is predicted for small patch sizes (in fact, there is a range of patch sizes where facilitation is predicted) and for sufficiently large patch sizes, while for intermediate patch sizes, predator-mediated exclusion of the prey is predicted by the model. As in the competitive case, we call this intermediate range of patch sizes a "dead zone" and note that the mechanism is again rooted in the increased prey emigration due to the presence of the predator leading to increased mortality experienced in the hostile matrix overcoming the prey's reproductive ability.

3. Preliminaries

In this section, we present some mathematical preliminaries that will be extensively used in the proofs of our main results.

3.1. Coupled sub–supersolutions

We use the method of sub–supersolutions to prove existence of positive solutions.

When g and h are increasing functions, then $\Psi = (\psi_1, \psi_2)$ and $\Phi = (z_1, z_2)$ in $C^2(\Omega) \cap C^1(\overline{\Omega})$ are called a coupled subsolution and supersolution of (1.3) if they satisfy

$$\begin{cases} -\Delta\psi_1 \leq \lambda\psi_1(1-\psi_1);\ \Omega \\ -\Delta\psi_2 \leq \lambda r\psi_2(1-\psi_2);\ \Omega \\ \frac{\partial\psi_1}{\partial\eta} + \sqrt{\lambda}g(z_2)\psi_1 \leq 0;\ \partial\Omega \\ \frac{\partial\psi_2}{\partial\eta} + \sqrt{\lambda}h(z_1)\psi_2 \leq 0;\ \partial\Omega \end{cases} \tag{3.1}$$

$$\begin{cases} -\Delta z_1 \geq \lambda z_1(1-z_1);\ \Omega \\ -\Delta z_2 \geq \lambda r z_2(1-z_2);\ \Omega \\ \frac{\partial z_1}{\partial \eta} + \sqrt{\lambda} g(\psi_2) z_1 \geq 0;\ \partial\Omega \\ \frac{\partial z_2}{\partial \eta} + \sqrt{\lambda} h(\psi_1) z_2 \geq 0;\ \partial\Omega. \end{cases} \tag{3.2}$$

When g is increasing and h is decreasing, then $\Psi = (\psi_1, \psi_2)$ and $\Phi = (z_1, z_2)$ in $C^2(\Omega) \cap C^1(\overline{\Omega})$ are called a coupled subsolution and supersolution of (1.3) if they satisfy

$$\begin{cases} -\Delta \psi_1 \leq \lambda \psi_1(1-\psi_1);\ \Omega \\ -\Delta \psi_2 \leq \lambda r \psi_2(1-\psi_2);\ \Omega \\ \frac{\partial \psi_1}{\partial \eta} + \sqrt{\lambda} g(z_2) \psi_1 \leq 0;\ \partial\Omega \\ \frac{\partial \psi_2}{\partial \eta} + \sqrt{\lambda} h(\psi_1) \psi_2 \leq 0;\ \partial\Omega \end{cases} \tag{3.3}$$

$$\begin{cases} -\Delta z_1 \geq \lambda z_1(1-z_1);\ \Omega \\ -\Delta z_2 \geq \lambda r z_2(1-z_2);\ \Omega \\ \frac{\partial z_1}{\partial \eta} + \sqrt{\lambda} g(\psi_2) z_1 \geq 0;\ \partial\Omega \\ \frac{\partial z_2}{\partial \eta} + \sqrt{\lambda} h(z_1) z_2 \geq 0;\ \partial\Omega. \end{cases} \tag{3.4}$$

Then the following result holds for both cases (See Theorem 9.8.2 in [33]).

Lemma 3.1. *Let $\Psi = (\psi_1, \psi_2)$ and $\Phi = (z_1, z_2)$ be a coupled subsolution and supersolution of* (1.3)*, respectively, such that $(\psi_1, \psi_2) \leq (z_1, z_2)$ and $\Psi, \Phi \in [C^2(\Omega) \cap C^1(\overline{\Omega})] \times [C^2(\Omega) \cap C^1(\overline{\Omega})]$. Then* (1.3) *has a solution $(u, v) \in [C^2(\Omega) \cap C^1(\overline{\Omega})] \times [C^2(\Omega) \cap C^1(\overline{\Omega})]$ such that $(\psi_1, \psi_2) \leq (u, v) \leq (z_1, z_2)$; $\overline{\Omega}$.*

3.2. Quadrature method

In the one-dimensional case, (1.3) reduces to the following system:

$$\begin{cases} -u'' = \lambda u(1-u);\ (0,1) \\ -v'' = \lambda r v(1-v);\ (0,1) \\ -u'(0) + \sqrt{\lambda} g(v(0)) u(0) = 0 \\ u'(1) + \sqrt{\lambda} g(v(1)) u(1) = 0 \\ -v'(0) + \sqrt{\lambda} h(u(0)) v(0) = 0 \\ v'(1) + \sqrt{\lambda} h(u(1)) v(1) = 0. \end{cases} \tag{3.5}$$

The following is an extension of a result which traces its origins to [34] with prototypical solution profiles for a positive solution of (3.5) given in Figure 20.

Theorem 3.1. *For a fixed $\lambda > 0$, with $g, h > 0$ as described in the hypotheses,* (1.3) *has a positive solution (u, v) if and only if there exist values of $u(0), v(0), u(1), v(1), \rho_u$, and ρ_v which satisfy $0 <$*

$u(0), u(1) < \rho_u < 1$, and $0 < v(0), v(1) < \rho_v < 1$, and the following:

$$\begin{cases} \sqrt{2\lambda} = \displaystyle\int_{u(0)}^{\rho_u} \frac{dz}{\sqrt{F(\rho_u) - F(z)}} + \int_{u(1)}^{\rho_u} \frac{dz}{\sqrt{F(\rho_u) - F(z)}} \\ \sqrt{2\lambda} = \displaystyle\int_{v(0)}^{\rho_v} \frac{dz}{\sqrt{r[F(\rho_v) - F(z)]}} + \int_{v(1)}^{\rho_v} \frac{dz}{\sqrt{r[F(\rho_v) - F(z)]}} \\ [g(v(0))u(0)]^2 = 2[F(\rho_u) - F(u(0))] \\ [g(v(1))u(1)]^2 = 2[F(\rho_u) - F(u(1))] \\ [h(u(0))v(0)]^2 = 2r[F(\rho_v) - F(v(0))] \\ [h(u(1))v(1)]^2 = 2r[F(\rho_v) - F(v(1))], \end{cases} \tag{3.6}$$

where $F(z) = \int_0^z s(1-s)ds$.

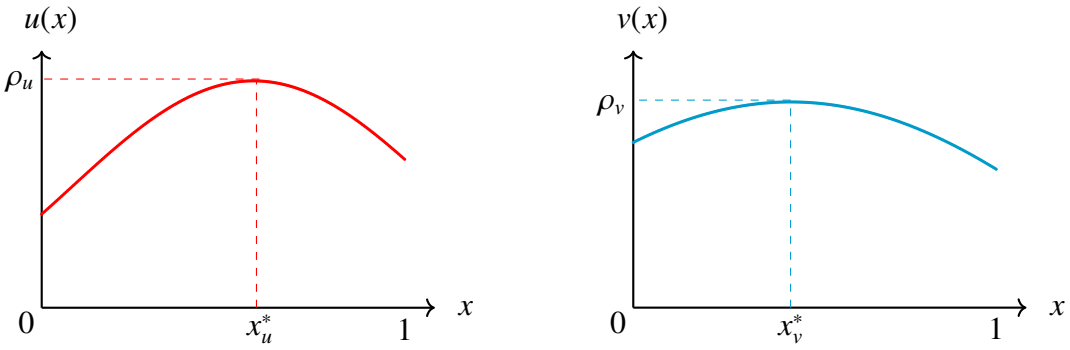

(a) u with maximum at x_u^*. **(b)** v with maximum at x_v^*.

Figure 20. Prototypical profiles of the solution components u and v.

Remark 3.1. *The proof of Theorem 2.3 is provided in the Appendix.*

We make use of this quadrature method to produce bifurcation curves, which, in turn, provides motivation for the theoretical results. For implementation, we utilize MATLAB (MathWorks, Inc. version 2023b). We construct a vector of ρ_u values and then generate a set of initial guesses of the form $(\rho_v, u(0), v(0), u(1), v(1))$ which are passed to `fsolve`; intermediate calculations require the use of `integral`. Using the output `exitflag` and a tolerance of 10^{-9} to check for convergence, we store the numeric solutions of (3.6) and recover the corresponding values of λ. Each bifurcation curve is a collection of points (λ, ρ).

4. Proofs of analytical results

In this section, we present proofs of our main results.

4.1. Proofs for Case 1: Trait–mediated competition

We first state and prove a lemma regarding the ordering of $\tilde{w}_1, \tilde{w}_2$ and any positive solution (u, v) of (1.3).

Lemma 4.1. *If (u, v) is a positive solution of (1.3) for $\lambda > \lambda^{0,0}$, then we must have*

$$\begin{aligned} u &< \tilde{w}_1;\ \overline{\Omega} \\ v &< \tilde{w}_2;\ \overline{\Omega}, \end{aligned} \tag{4.1}$$

where $\tilde{w}_1(x)$ and $\tilde{w}_2(x)$ are the unique positive solutions of (2.2) and (2.3), respectively.

Proof of Lemma 4.1
Assume that (u, v) is a positive solution of (1.3) for $\lambda > \lambda^{0,0}$. We will show that u is a strict subsolution of (2.2). To that end, substituting u into (2.2) gives

$$\begin{cases} -\Delta u - \lambda u(1-u) = 0;\ \Omega \\ \frac{\partial u}{\partial \eta} + \sqrt{\lambda} g(0) u = -\sqrt{\lambda} g(v) u + \sqrt{\lambda} g(0) u = \sqrt{\lambda} u\,(g(0) - g(v)) < 0;\ \partial\Omega, \end{cases}$$

since g is increasing and v is positive. The uniqueness of $\tilde{w}_1(x)$ then guarantees that $u < \tilde{w}_1(x);\ \overline{\Omega}$. An almost identical argument for v gives $v < \tilde{w}_2(x);\ \overline{\Omega}$.

Next, we present the proofs for Theorems 2.1–2.3.

Proof of Theorem 2.1

(a) By (2.9), for $\lambda = E_1(1, g(0))$, we have $\mu_1(\sqrt{E_1(1, g(0))} g(0)) = E_1(1, g(0))$. Moreover, by (2.10), for $\lambda = E_1(r, h(0))$, we have $\mu_1(\sqrt{E_1(r, h(0))} h(0)) = r E_1(r, h(0))$. Since $\mu_1(\sqrt{\lambda}\gamma)$ is concave for any fixed $\gamma > 0$, $\mu_1(\sqrt{\lambda} g(0)) > \lambda$ for $\lambda < E_1(1, g(0))$ and $\mu_1(\sqrt{\lambda} h(0)) > \lambda r$ for $\lambda < E_1(r, h(0))$. Then (2.9) and (2.10) imply that $\sigma_1 \geq 0$ for $\lambda \leq E_1(1, g(0))$ (see Figure 21) and $\sigma_2 \geq 0$ for $\lambda \leq E_1(r, h(0))$ (see Figure 22).

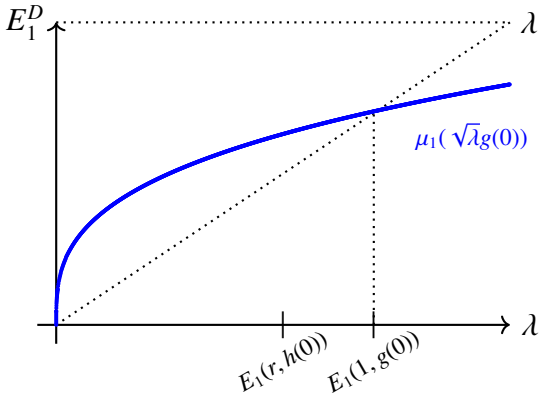

Figure 21. Eigencurve diagram to illustrate that $\sigma_1 \geq 0$ for $\lambda \leq E_1(1, g(0))$ when $E_1(r, h(0)) \leq E_1(1, g(0))$.

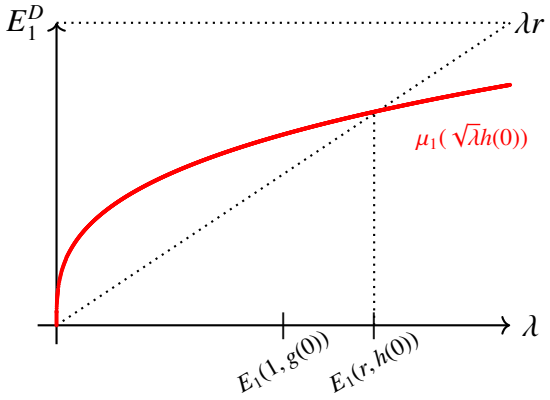

Figure 22. Eigencurve diagram to illustrate that $\sigma_2 \geq 0$ for $\lambda \leq E_1(r, h(0))$ when $E_1(1, g(0)) \leq E_1(r, h(0))$.

By way of contradiction, suppose that (u, v) is a positive solution of (1.3) for $\lambda < \lambda^{0,0}$.

Case 1: $E_1(r, h(0)) \leq E_1(1, g(0))$
By Green's second identity, we know that

$$\int_\Omega \Big(\Delta\phi_1 u - \Delta u\phi_1\Big)dx = \int_{\partial\Omega} \left(\frac{\partial\phi_1}{\partial\eta}u - \frac{\partial u}{\partial\eta}\phi_1\right) ds.$$

Now, using the fact $\sigma_1 \geq 0$ for $\lambda \leq E_1(1, g(0))$, we have

$$\begin{aligned}\int_\Omega \Big(\Delta\phi_1 u - \Delta u\phi_1\Big)dx &= \int_\Omega (-\lambda\phi_1 u - \sigma_1\phi_1 u + \lambda\phi_1 u - \lambda\phi_1 u^2)dx \\ &= -\int_\Omega u\phi_1(\sigma_1 + \lambda u)dx \leq 0.\end{aligned}$$

However, since g is increasing, we have

$$\begin{aligned}\int_{\partial\Omega} \left(\frac{\partial\phi_1}{\partial\eta}u - \frac{\partial u}{\partial\eta}\phi_1\right) ds &= \int_{\partial\Omega} \Big(-\sqrt{\lambda}g(0)\phi_1 u + \sqrt{\lambda}g(v)u\phi_1\Big)\, ds \\ &= \int_{\partial\Omega} \sqrt{\lambda}u\phi_1\Big(g(v) - g(0)\Big)ds > 0,\end{aligned}$$

which is a contradiction. Hence, (1.3) has no positive solution for $\lambda \leq E_1(1, g(0))$.

Case 2: $E_1(1, g(0)) \leq E_1(r, h(0))$
By a similar argument, since $\sigma_2 \geq 0$ for $\lambda \leq E_1(r, h(0))$, we have

$$\begin{aligned}\int_\Omega \Big(\Delta\phi_2 v - \Delta v\phi_2\Big)dx &= \int_\Omega (-\lambda r\phi_2 v - \sigma_2\phi_2 v + \lambda r\phi_2 v - \lambda r\phi_2 v^2)dx \\ &= -\int_\Omega v\phi_2(\sigma_2 + \lambda v)dx \leq 0.\end{aligned}$$

However, since h is increasing, we have

$$\int_{\partial\Omega}\Big(\frac{\partial\phi_2}{\partial\eta}v-\frac{\partial v}{\partial\eta}\phi_2\Big)ds=\int_{\partial\Omega}\Big(-\sqrt{\lambda}h(0)v\phi_2+\sqrt{\lambda}h(u)v\phi_2\Big)\,ds$$
$$=\int_{\partial\Omega}\sqrt{\lambda}v\phi_2\,(h(u)-h(0))\,ds>0,$$

which is a contradiction. Hence, (1.3) has no positive solution for $\lambda\le E_1(r,h(0))$.

Combining the two cases, we conclude that (1.3) has no positive solution for $\lambda\le\lambda^{0,0}$.

(b) For a fixed $\lambda > E_1(1,g(1))$, let w_1^* be the unique positive solution of (2.14), and for a fixed $\lambda > E_1(r,h(1))$, let w_2^* be the unique positive solution of (2.15). Hence, w_1^*, w_2^* both exist for $\lambda>\lambda^{1,1}$ and satisfy $w_1^*, w_2^* < 1;\ \overline{\Omega}$. Consider $(\psi_1,\psi_2)=(w_1^*,w_2^*)$ and $(z_1,z_2)=(1,1)$. Since g and h are increasing, we have

$$\begin{cases}
-\Delta\psi_1=-\Delta w_1^*=\lambda w_1^*(1-w_1^*)=\lambda\psi_1(1-\psi_1);\ \Omega\\
-\Delta\psi_2=-\Delta w_2^*=\lambda r w_2^*(1-w_2^*)=\lambda r\psi_2(1-\psi_2);\ \Omega\\
\frac{\partial\psi_1}{\partial\eta}+\sqrt{\lambda}g(z_2)\psi_1=\frac{\partial w_1^*}{\partial\eta}+\sqrt{\lambda}g(1)w_1^*=0;\ \partial\Omega\\
\frac{\partial\psi_2}{\partial\eta}+\sqrt{\lambda}h(z_1)\psi_2=\frac{\partial w_2^*}{\partial\eta}+\sqrt{\lambda}h(1)w_2^*=0;\ \partial\Omega\\
-\Delta z_1=-\Delta(1)=0=\lambda(1)(1-1)=\lambda z_1(1-z_1);\ \Omega\\
-\Delta z_2=-\Delta(1)=0=\lambda r(1)(1-1)=\lambda r z_2(1-z_2);\ \Omega\\
\frac{\partial z_1}{\partial\eta}+\sqrt{\lambda}g(\psi_2)z_1=\frac{\partial 1}{\partial\eta}+\sqrt{\lambda}g(w_2^*)(1)>0;\ \partial\Omega\\
\frac{\partial z_2}{\partial\eta}+\sqrt{\lambda}h(\psi_1)z_2=\frac{\partial 1}{\partial\eta}+\sqrt{\lambda}h(w_1^*)(1)>0;\ \partial\Omega.
\end{cases}$$

Since $(w_1^*,w_2^*)<(1,1)$, by applying Lemma 3.1, (1.3) has a positive solution (u,v) satisfying $(w_1^*,w_2^*)<(u,v)<(1,1)$ for $\lambda>\lambda^{1,1}$.

(c) Lemma 4.1 gives this result immediately.

Proof of Theorem 2.2

Let $r<r^*$, which implies that $E_1(1,g(0))<E_1(r,h(0))$. From Theorem 1 on page 5 of [31], we have $\tilde{w}_2\to 0;\ \overline{\Omega}$ as $\lambda\to E_1(r,h(0))^+$ and $\tilde{w}_1>0;\ \overline{\Omega}$ for all $\lambda>E_1(1,g(0))$. If (u,v) is a positive solution of (1.3) for $\lambda\in[E_1(r,h(0)),E_1(r,h(1))]$, then Lemma 4.1 gives $v<\tilde{w}_2;\ \overline{\Omega}$ implying that $v\to 0;\ \overline{\Omega}$ as $\lambda\to E_1(r,h(0))^+$. A standard compactness argument now gives $u\to\tilde{w}_1;\ \overline{\Omega}$ as $\lambda\to E_1(r,h(0))^+$. This, combined with the fact that $\tilde{w}_1>0;\ \overline{\Omega}$ for $\lambda=E_1(r,h(0))$, implies that $\epsilon,\xi>0$ with $\epsilon,\xi\approx 0$ must exist such that $u\ge\epsilon;\ \overline{\Omega}$ for $\lambda\in[E_1(r,h(0)),E_1(r,h(0))+\xi]$. Now we choose $\xi_1>0$, $\xi_1\approx 0$ such that $\xi_1<\xi$ and $E_1(r,h(0))+\xi_1<E_1(r,h(\epsilon))$.

Next, assume that (u,v) is a positive solution of (1.3) for $\lambda\in[E_1(r,h(0)),E_1(r,h(0))+\xi_1]$ and consider $a\equiv\epsilon$ in the principal eigenvalue $\sigma_3(\epsilon)$ of (2.6). It is easy to see that $\sigma_3(\epsilon)>0$ for $\lambda\in(0,E_1(r,h(\epsilon)))$. Since h is increasing and $\tilde{w}_1<1;\ \overline{\Omega}$, we have $E_1(r,h(0))<E_1(r,h(\epsilon))<E_1(r,h(1))$. Now, from Green's second identity, we have

$$\int_\Omega\Big(\Delta v\phi_3-\Delta\phi_3 v\Big)dx=\int_{\partial\Omega}\left(\frac{\partial v}{\partial\eta}\phi_3-\frac{\partial\phi_3}{\partial\eta}v\right)ds.$$

Using the fact that $\sigma_3(\epsilon) > 0$, we have

$$\begin{aligned}\int_\Omega \Big(\Delta v\phi_3 - \Delta\phi_3 v\Big)dx &= \int_\Omega \Big(- \lambda rv(1-v)\phi_3 + (\lambda r + \sigma_3)\phi_3 v\Big)dx \\ &= \int_\Omega \Big(- \lambda rv\phi_3 + \lambda rv^2\phi_3 + \lambda r\phi_3 v + \sigma_3\phi_3 v\Big)dx \\ &= \int_\Omega \phi_3 v\Big(\lambda rv + \sigma_3\Big)dx > 0.\end{aligned}$$

On the other hand, since $u \geq \epsilon$; $\overline{\Omega}$ and h is increasing, combined with $\sigma_3(\epsilon) > 0$, we have

$$\begin{aligned}\int_{\partial\Omega}\left(\frac{\partial v}{\partial\eta}\phi_3 - \frac{\partial\phi_3}{\partial\eta}v\right)ds &= \int_{\partial\Omega}\left(-\sqrt{\lambda}h(u)v\phi_3 - \left(\sigma_3 - \sqrt{\lambda}h(\epsilon)\right)\phi_3 v\right)ds \\ &= \int_{\partial\Omega}\phi_3 v\Big(- \sigma_3 + \sqrt{\lambda}\left[h(\epsilon) - h(u)\right]\Big)ds < 0.\end{aligned}$$

This leads to a contradiction, and hence (1.3) has no positive solution in $\Big[E_1(r, h(0)), E_1(r, h(0)) + \xi_1\Big]$.

Proof of Theorem 2.3

An almost identical argument to that in the proof of Theorem 2.2 gives this result and is hence left to the interested reader.

4.2. Proofs for Case 2: Non–consumptive predator–prey

In this subsection, we present the proofs of our main results for the non–consumptive predator–prey case.

Proof of Theorem 2.4

(a) To prove nonexistence, we consider two cases.

Case 1: $E_1(1, g(0)) \geq E_1(r, h(1))$

By way of contradiction, suppose that (u, v) is a positive solution of (1.3) for a fixed $\lambda > 0$ satisfying $\lambda \leq E_1(1, g(0))$. Then, by using a similar argument as in Theorem 2.1, $\sigma_1 \geq 0$ for $\lambda \leq E_1(1, g(0))$. Applying Green's second identity, we have

$$\int_\Omega \Big(- \Delta u\phi_1 + \Delta\phi_1 u\Big)dx = \int_{\partial\Omega}\Big(- \frac{\partial u}{\partial\eta}\phi_1 + \frac{\partial\phi_1}{\partial\eta}u\Big)ds.$$

Now, since $\sigma_1 \geq 0$ for $\lambda \leq E_1(1, g(0))$, we have

$$\begin{aligned}\int_\Omega \Big(- \Delta u\phi_1 + \Delta\phi_1 u\Big)dx &= \int_\Omega \Big(\lambda u(1-u)\phi_1 - (\lambda + \sigma_1)\phi_1 u\Big)dx \\ &= \int_\Omega \Big(\lambda u\phi_1 - \lambda u^2\phi_1 - \lambda\phi_1 u - \sigma_1\phi_1 u\Big)dx \\ &= - \int_\Omega u\phi_1(\sigma_1 + \lambda u)dx \leq 0.\end{aligned}$$

On the other hand, since g is increasing and $v > 0;\ \overline{\Omega}$, we have

$$\int_{\partial\Omega}\Big(-\frac{\partial u}{\partial\eta}\phi_1+\frac{\partial\phi_1}{\partial\eta}u\Big)ds=\int_{\partial\Omega}\sqrt{\lambda}\phi_1 u\Big(g(v)-g(0)\Big)ds>0.$$

This gives a contradiction. Thus, no positive solution of (1.3) exists for $\lambda \le E_1(1, g(0))$.

Case 2: $E_1(r, h(1)) \ge E_1(1, g(0))$

Letting $a \equiv 1$, consider the principal eigenvalue $\sigma_3(1)$ of (2.6) and let $\phi_3 > 0;\ \overline{\Omega}$ be the corresponding normalized eigenfunction. By way of contradiction, suppose that (u, v) is a positive solution of (1.3) for a fixed $\lambda > 0$ satisfying $\lambda \le E_1(r, h(1))$. Note that $\sigma_3(1) \ge 0$ for $\lambda \le E_1(r, h(1))$. Applying Green's second identity, we have

$$\int_\Omega\Big(\Delta v\phi_3-\Delta\phi_3 v\Big)dx=\int_{\partial\Omega}\Big(\frac{\partial v}{\partial\eta}\phi_3-\frac{\partial\phi_3}{\partial\eta}v\Big)ds.$$

Since $\sigma_3 \ge 0$ for $\lambda \le E_1(r, h(1))$, we have

$$\begin{aligned}\int_\Omega\Big(\Delta v\phi_3-\Delta\phi_3 v\Big)dx&=\int_\Omega\Big(-\lambda rv(1-v)\phi_3+(\lambda r+\sigma_3)\phi_3 v\Big)dx\\&=\int_\Omega\Big(-\lambda rv\phi_3+\lambda rv^2\phi_3+\lambda r\phi_3 v+\sigma_3\phi_3 v\Big)dx\\&=\int_\Omega v\phi_3(\sigma_3+\lambda rv)dx\ge 0.\end{aligned}$$

On the other hand, since h is decreasing, we have

$$\int_{\partial\Omega}\Big(\frac{\partial v}{\partial\eta}\phi_3-\frac{\partial\phi_3}{\partial\eta}v\Big)ds=\int_{\partial\Omega}\phi_3 v\Big(-\sigma_3+\sqrt{\lambda}\,(h(1)-h(u))\Big)ds<0.$$

This gives a contradiction, so no positive solution of (1.3) exists for $\lambda \le E_1(r, h(1))$.

Combining these results, we see that (1.3) has no positive solution for $\lambda \le \lambda^{0,1}$.

(b) Recall that the unique positive solution of (2.3), $\tilde{w}_2$, exists for $\lambda > E_1(r, h(0))$ and the unique positive solution of (2.14), w_1^*, exists for $\lambda > E_1(1, g(1))$. Hence, both exist when $\lambda > \lambda^{1,0}$. Moreover, $w_1^*, \tilde{w}_2 < 1;\ \overline{\Omega}$. Take $(\psi_1, \psi_2) = (w_1^*, \tilde{w}_2)$ and $(z_1, z_2) = (1, 1)$. Since g is increasing, and h is decreasing, we have

$$\begin{cases}-\Delta\psi_1=-\Delta w_1^*=\lambda w_1^*(1-w_1^*)=\lambda\psi_1(1-\psi_1);\ \Omega\\ -\Delta\psi_2=-\Delta\tilde{w}_2=\lambda r\tilde{w}_2(1-\tilde{w}_2)=\lambda r\psi_2(1-\psi_2);\ \Omega\\ \frac{\partial\psi_1}{\partial\eta}+\sqrt{\lambda}g(z_2)\psi_1=\frac{\partial w_1^*}{\partial\eta}+\sqrt{\lambda}g(1)w_1^*=0;\ \partial\Omega\\ \frac{\partial\psi_2}{\partial\eta}+\sqrt{\lambda}h(\psi_1)\psi_2=\frac{\partial\tilde{w}_2}{\partial\eta}+\sqrt{\lambda}h(w_1^*)\tilde{w}_2\le\frac{\partial\psi_2}{\partial\eta}+\sqrt{\lambda}h(0)\psi_2=0;\ \partial\Omega\\ -\Delta z_1=-\Delta 1=0=\lambda(1)(1-1)=\lambda z_1(1-z_1);\ \Omega\\ -\Delta z_2=-\Delta 1=0=\lambda r(1)(1-1)=\lambda r z_2(1-z_2);\ \Omega\\ \frac{\partial z_1}{\partial\eta}+\sqrt{\lambda}g(\psi_2)z_1=\frac{\partial(1)}{\partial\eta}+\sqrt{\lambda}g(\tilde{w}_2)(1)>0;\ \partial\Omega\\ \frac{\partial z_2}{\partial\eta}+\sqrt{\lambda}h(z_1)z_2=\frac{\partial(1)}{\partial\eta}+\sqrt{\lambda}h(1)(1)>0;\ \partial\Omega.\end{cases}$$

Since $(w_1^*, \tilde{w}_2) \leq (1,1)$, applying Lemma 3.1, (1.3) has a positive solution (u,v) satisfying $(w_1^*, \tilde{w}_2) \leq (u,v) \leq (1,1)$ for $\lambda > \lambda^{1,0}$.

(c) Assume that (u,v) is a positive solution of (1.3) for $\lambda > \lambda^{0,1}$. Since g is increasing, as in the competition case, Lemma 4.1 immediately gives $0 < u < \tilde{w}_1;\ \overline{\Omega}$, where $\tilde{w}_1$ is the unique positive solution of (2.2). Moreover, since $\lambda > E_1(r, h(1))$, the unique positive solution, w_2^*, of (2.15) exists. We will now show that v is a strict subsolution of (2.15). To that end, we substitute v into (2.15) and calculate

$$\begin{cases} -\Delta v - \lambda r v(1-v) = 0;\ \Omega \\ \frac{\partial v}{\partial \eta} + \sqrt{\lambda} h(1) v = -\sqrt{\lambda} h(u) v + \sqrt{\lambda} h(1) v = \sqrt{\lambda} v\,(h(1) - h(u)) < 0;\ \partial\Omega \end{cases}$$

since h is decreasing and $u < 1;\ \overline{\Omega}$. The uniqueness of w_2^* then guarantees that $v < w_2^*;\ \overline{\Omega}$. In the case where $\lambda > E_1(r, h(0))$, the unique positive solution of (2.3) exists, and an almost identical argument shows that v is a strict supersolution of (2.3). This, combined with the uniqueness of the positive solution of (2.3), gives $\tilde{w}_2 < v < w_2^*;\ \overline{\Omega}$.

Proof of Theorem 2.5

Assume that $r < r^*$, which implies that $E_1(1, g(0)) < E_1(r, h(0))$.

(a) Assume that $\lambda^{0,1} = E_1(r, h(1))$ and $\lambda^{1,0} = E_1(1, g(1))$. Note that for $\lambda > \lambda^{0,1}$, the unique positive solution, $\tilde{w}_1$, of (2.2) exists and satisfies $\tilde{w}_1 < 1;\ \overline{\Omega}$. Thus, for a fixed $\lambda \in \left[E_1(1, g(0)), \lambda^{1,0}\right]$, an $\epsilon > 0$ with $\epsilon \approx 0$ must exist such that $\tilde{w}_1 < 1 - \epsilon;\ \overline{\Omega}$. When $a \equiv 1 - \epsilon$, recall that the principal eigenvalue $\sigma_3(1-\epsilon)$ of (2.6) satisfies $\sigma_3(1-\epsilon) > 0$ for $\lambda < E_1(r, h(1-\epsilon))$. Moreover, a decreasing h implies that a $\xi_1 > 0$ exists such that $E_1(r, h(1)) < E_1(r, h(1-\epsilon)) = E_1(r, h(1)) + \xi_1$. Now, assume that (u,v) is a positive solution of (1.3) for $\lambda \in [\lambda^{0,1}, \lambda^{0,1} + \xi_1)$. Lemma 4.1 gives $u < \tilde{w}_1;\ \overline{\Omega}$. Using Green's second identity, we have

$$\int_\Omega \Big(\Delta v \phi_3 - \Delta \phi_3 v\Big) dx = \int_{\partial\Omega} \left(\frac{\partial v}{\partial \eta}\phi_3 - \frac{\partial \phi_3}{\partial \eta} v\right) ds.$$

Using the fact that $\sigma_3(1-\epsilon) > 0$, we have

$$\begin{aligned} \int_\Omega \Big(\Delta v \phi_3 - \Delta \phi_3 v\Big) dx &= \int_\Omega \Big(-\lambda r v(1-v)\phi_3 + (\lambda r + \sigma_3)\phi_3 v\Big) dx \\ &= \int_\Omega \Big(-\lambda r v \phi_3 + \lambda r v^2 \phi_3 + \lambda r \phi_3 v + \sigma_3 \phi_3 v\Big) dx \\ &= \int_\Omega \phi_3 v \Big(\lambda r v + \sigma_3\Big) dx > 0. \end{aligned}$$

On the other hand, a decreasing h combined with $\sigma_3(1-\epsilon) > 0$ and $u < \tilde{w}_1 < 1 - \epsilon;\ \overline{\Omega}$ gives

$$\begin{aligned} \int_{\partial\Omega} \left(\frac{\partial v}{\partial \eta}\phi_3 - \frac{\partial \phi_3}{\partial \eta} v\right) ds &= \int_{\partial\Omega} \Big(-\sqrt{\lambda} h(u) v \phi_3 - \Big(\sigma_3 - \sqrt{\lambda} h(1-\epsilon)\Big)\phi_3 v\Big)\, ds \\ &= \int_{\partial\Omega} \phi_3 v \Big(-\sigma_3 + \sqrt{\lambda}\,[h(1-\epsilon) - h(u)]\Big)\, ds \\ &< \int_{\partial\Omega} \phi_3 v \Big(-\sigma_3 + \sqrt{\lambda}\,[h(1-\epsilon) - h(\tilde{w}_1)]\Big)\, ds < 0. \end{aligned}$$

This leads to a contradiction, and hence (1.3) has no positive solution in $[E_1(r, h(0)), E_1(r, h(0)) + \xi_1]$.

(b) Assume that $\lambda^{0,1} = E_1(r, h(1))$ and $\lambda^{1,0} = E_1(1, g(1))$. For nonexistence, the argument in (a) above can be followed but with a potentially different ξ-value (say, $\xi_2 > 0$ and $\xi_2 \approx 0$). For coexistence, note that $\lambda > \lambda^{1,0}$ implies that the unique positive solution w_1^* of (2.14) exists, and we can define σ_3^* as the principal eigenvalue of

$$\begin{cases} -\Delta\phi = (\lambda r + \sigma)\phi; \ \Omega \\ \frac{\partial\phi}{\partial\eta} + \sqrt{\lambda}h(w_1^*)\phi = 0; \ \partial\Omega, \end{cases} \tag{4.2}$$

with the corresponding (normalized eigenfunction) $\phi_3^* > 0; \ \overline{\Omega}$.

Comparing (2.14) with (2.8), we obtain $\sigma_3^* = \mu_1(\sqrt{\lambda}h(w_1^*)) - \lambda r$. We claim that a $\delta_2 > 0$ exists such that $\sigma_3^* < 0$ for $\lambda \in \left(E_1(r, h(0)) - \delta_2, E_1(r, h(0))\right)$. Note that at $\lambda = E_1(r, h(0))$, we have $\mu_1(\sqrt{\lambda}h(0)) = r\lambda$. Since $\mu_1(\sqrt{\lambda}h(0))$ is concave, we know for $\lambda < E_1(r, h(0))$ that $\mu_1(\sqrt{\lambda}h(0)) > r\lambda$. In addition, h is decreasing, which implies $\mu_1(\sqrt{\lambda}h(w_1^*)) < \mu_1(\sqrt{\lambda}h(0))$ for $\lambda > E_1(1, g(1))$ and, in particular, for $\lambda \in \left(E_1(1, g(1)), E_1(r, h(0))\right]$. This implies the existence of a $\delta_2 > 0$ such that $\mu_1(\sqrt{\lambda}h(w_1^*)) = r\lambda$ at $\lambda = E_1(r, h(0)) - \delta_2$ and $\mu_1(\sqrt{\lambda}h(w_1^*)) < r\lambda$ for $\lambda \in \left(E_1(r, h(0)) - \delta_2, E_1(r, h(0))\right)$. Thus, $\sigma_3^* < 0$ for $\lambda \in \left(E_1(r, h(0)) - \delta_2, E_1(r, h(0))\right)$ and, more generally, for $\lambda > E_1(r, h(0)) - \delta_2$ (see Figure 23).

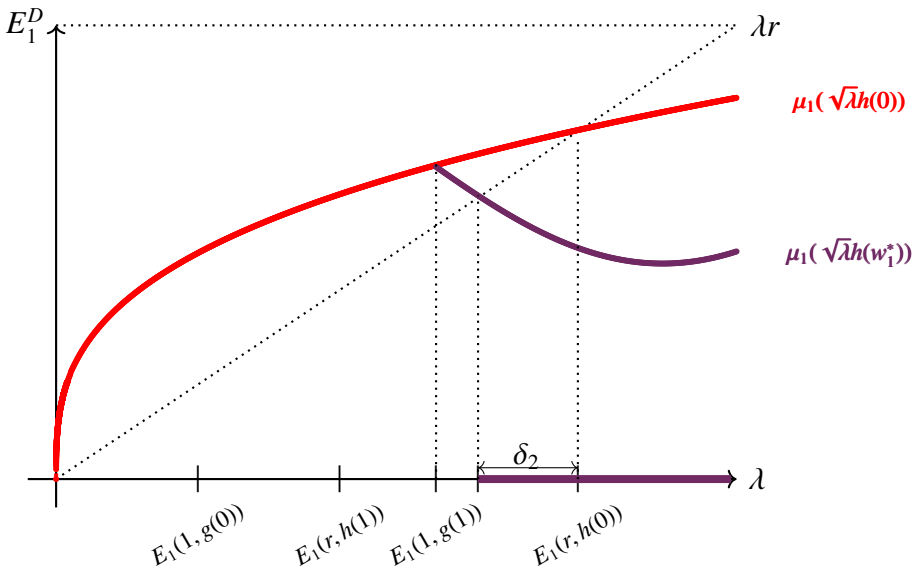

Figure 23. The eigencurve diagram illustrates that $\delta_2 > 0$ exists such that $\sigma_3^* < 0$ for $\lambda > E_1(r, h(0)) - \delta_2$.

Now, consider $(\psi_1, \psi_2) = (w_1^*, \epsilon\phi_3^*)$ and $(z_1, z_2) = (1, 1)$ as candidates for the coupled subsolution and supersolution of (1.3). Then

$$\begin{aligned} -\Delta\psi_1 - \lambda\psi_1(1 - \psi_1) &= -\Delta w_1^* - \lambda w_1^*(1 - w_1^*) \\ &= \lambda w_1^*(1 - w_1^*) - \lambda w_1^*(1 - w_1^*) \\ &= 0 \end{aligned}$$

$$\begin{aligned}-\Delta\psi_2 - \lambda r\psi_2(1-\psi_2) &= -\Delta\epsilon\phi_3^* - \lambda r\epsilon\phi_3^*(1-\epsilon\phi_3^*)\\ &= \epsilon\Big(-\Delta\phi_3^* - \lambda r\phi_3^*(1-\epsilon\phi_3^*)\Big)\\ &= \epsilon\Big((\lambda r+\sigma_3^*)\phi_3^* - \lambda r\phi_3^*(1-\epsilon\phi_3^*)\Big)\\ &= \epsilon\Big(\lambda r\phi_3^* + \sigma_3^*\phi_3^* - \lambda r\phi_3^* + \lambda r\epsilon(\phi_3^*)^2\Big)\\ &= \epsilon\phi_3^*(\sigma_3^* + \lambda r\epsilon\phi_3^*)\\ &\le 0,\end{aligned}$$

provided that $\sigma_3^* \le -\lambda r\epsilon\phi_3^*$. This is possible, since $\sigma_3^* < 0$ for $\lambda > E_1(r, h(0)) - \delta_2$ and we can take $\epsilon \approx 0$. Furthermore, we have

$$\begin{cases}\frac{\partial\psi_1}{\partial\eta} + \sqrt{\lambda}g(z_2)\psi_1 = \frac{\partial w_1^*}{\partial\eta} + \sqrt{\lambda}g(1)w_1^* = -\sqrt{\lambda}g(1)w_1^* + \sqrt{\lambda}g(1)w_1^* = 0\\ \frac{\partial\psi_2}{\partial\eta} + \sqrt{\lambda}h(\psi_1)\psi_2 = \frac{\partial\epsilon\phi_3^*}{\partial\eta} + \sqrt{\lambda}h(w_1^*)\epsilon\phi_3^* = \epsilon\Big(-\sqrt{\lambda}h(w_1^*)\phi_3^* + \sqrt{\lambda}h(w_1^*)\phi_3^*\Big) = 0\\ -\Delta z_1 - \lambda z_1(1-z_1) = -\Delta 1 - \lambda(1)(1-1) = 0\\ -\Delta z_2 - \lambda r z_2(1-z_2) = -\Delta 1 - \lambda r(1)(1-1) = 0\\ \frac{\partial z_1}{\partial\eta} + \sqrt{\lambda}g(\psi_2)z_1 = \frac{\partial(1)}{\partial\eta} + \sqrt{\lambda}g(\epsilon\phi_3^*)(1) = \sqrt{\lambda}g(\epsilon\phi_3^*) > 0.\\ \frac{\partial z_2}{\partial\eta} + \sqrt{\lambda}h(z_1)z_2 = \frac{\partial(1)}{\partial\eta} + \sqrt{\lambda}h(1)(1) = \sqrt{\lambda}h(1) > 0.\end{cases}$$

Thus, (ψ_1, ψ_2) and (z_1, z_2) are a coupled sub- and supersolution of (1.3) satisfying $(\psi_1, \psi_2) \le (z_1, z_2)$. Thus, by Lemma 3.1, a positive solution (u, v) exists such that $(w_1^*, \epsilon\phi_3^*) \le (u, v) \le (1, 1)$ for $\lambda > E_1(r, h(0)) - \delta_2$.

(c) Assume that $\lambda^{0,1} = E_1(1, g(0))$ and $\lambda^{1,0} = E_1(1, g(1))$. For $\lambda > \lambda^{0,1}$, the unique positive solution $\tilde{w}_1$ of (2.2) exists, and from Theorem 1(a) on page 5 of [31], satisfies $\|\tilde{w}_1\|_\infty \to 0$ as $\lambda \to E_1(1, g(0))^+$. Letting $a \equiv 0$, $E_1(1, g(0)) < E_1(r, h(0))$ implies that the principal eigenvalue $\sigma_3(0)$ of (2.6) satisfies $\sigma_3(0) > 0$ for $\lambda \in \Big[\lambda^{0,1}, E_1(r, h(0))\Big)$. Thus, we can find a $\xi_3 > 0$ with $\xi_3 \approx 0$ such that for $\lambda \in \Big[\lambda^{0,1}, \lambda^{0,1} + \xi_3\Big]$, we have

$$-\sigma_3 + \sqrt{\lambda}\,(h(0) - h(\tilde{w}_1)) < 0;\ \overline{\Omega}. \tag{4.3}$$

Now, assume (u, v) is a positive solution of (1.3) for $\lambda \in [\lambda^{0,1}, \lambda^{0,1} + \xi_3]$. Using Green's second identity, we have

$$\int_\Omega \Big(\Delta v\phi_3 - \Delta\phi_3 v\Big)dx = \int_{\partial\Omega}\left(\frac{\partial v}{\partial\eta}\phi_3 - \frac{\partial\phi_3}{\partial\eta}v\right)ds.$$

Using the fact that $\sigma_3(0) > 0$, we have

$$\begin{aligned}\int_\Omega \Big(\Delta v\phi_3 - \Delta\phi_3 v\Big)dx &= \int_\Omega \Big(-\lambda rv(1-v)\phi_3 + (\lambda r+\sigma_3)\phi_3 v\Big)dx\\ &= \int_\Omega \Big(-\lambda rv\phi_3 + \lambda rv^2\phi_3 + \lambda r\phi_3 v + \sigma_3\phi_3 v\Big)dx\\ &= \int_\Omega \phi_3 v\Big(\lambda rv + \sigma_3\Big)dx > 0.\end{aligned}$$

On the other hand, a decreasing h combined with $u < \tilde{w}_1;\ \overline{\Omega}$ and (4.3) gives

$$\begin{aligned}\int_{\partial\Omega}\left(\frac{\partial v}{\partial \eta}\phi_3 - \frac{\partial \phi_3}{\partial \eta}v\right)ds &= \int_{\partial\Omega}\left(-\sqrt{\lambda}h(u)v\phi_3 - \left(\sigma_3 - \sqrt{\lambda}h(0)\right)\phi_3 v\right)ds\\ &= \int_{\partial\Omega}\phi_3 v\left(-\sigma_3 + \sqrt{\lambda}\left[h(0) - h(u)\right]\right)ds\\ &< \int_{\partial\Omega}\phi_3 v\left(-\sigma_3 + \sqrt{\lambda}\left[h(0) - h(\tilde{w}_1)\right]\right)ds < 0.\end{aligned}$$

This leads to a contradiction, and hence (1.3) has no positive solution in $\left[\lambda^{0,1}, \lambda^{0,1} + \xi_3\right]$.

(d) The arguments from (b) and (c) can be applied but with potentially different δ- and ξ-values (say $\delta_4, \xi_4 > 0$ with $\delta_4, \xi_4 \approx 0$).

Proof of Theorem 2.6

Assume that $r > r^*$, implying that $E_1(r, h(0)) < E_1(1, g(0))$. Then $\lambda^{0,1} = E_1(1, g(0))$ and $\lambda^{1,0} = E_1(1, g(1))$. For $\lambda > \lambda^{0,1}$, the unique positive solution $\tilde{w}_2$ of (2.3) exists and satisfies $\tilde{w}_2 > 0;\ \overline{\Omega}$. Thus, an $\epsilon > 0$ exists such that for $\lambda \in \left[\lambda^{0,1}, \lambda^{1,0}\right]$, we must have $\tilde{w}_2 > \epsilon;\ \overline{\Omega}$. Letting $a \equiv \epsilon$, the principal eigenvalue $\sigma_4(\epsilon)$ of (2.7) satisfies $\sigma_4(\epsilon) > 0$ for $\lambda \in (0, E_1(1, g(\epsilon)))$. Moreover, an increasing g implies that $\lambda^{0,1} = E_1(1, g(0)) < E_1(1, g(\epsilon))$ and there is a $\xi_5 > 0$ with $\xi_5 \approx 0$ such that $\sigma_4(\epsilon) > 0$ for $\lambda \in \left[\lambda^{0,1}, \lambda^{0,1} + \xi_5\right]$. Assume that (u, v) is a positive solution of (1.3) for $\lambda \in \left[\lambda^{0,1}, \lambda^{0,1} + \xi_5\right]$. Using Green's second identity, we have

$$\int_\Omega \left(\Delta u\phi_4 - \Delta\phi_4 u\right)dx = \int_{\partial\Omega}\left(\frac{\partial u}{\partial \eta}\phi_4 - \frac{\partial \phi_4}{\partial \eta}u\right)ds.$$

Using the fact that $\sigma_4(0) > 0$, we have

$$\begin{aligned}\int_\Omega \left(\Delta u\phi_4 - \Delta\phi_4 u\right)dx &= \int_\Omega \left(-\lambda u(1-u)\phi_4 + (\lambda + \sigma_4)\phi_4 u\right)dx\\ &= \int_\Omega \left(-\lambda u\phi_4 + \lambda u^2\phi_4 + \lambda\phi_4 u + \sigma_4\phi_4 u\right)dx\\ &= \int_\Omega \phi_4 u\left(\lambda u + \sigma_4\right)dx > 0.\end{aligned}$$

On the other hand, an increasing g combined with $\epsilon < \tilde{w}_2;\ \overline{\Omega}$ gives

$$\begin{aligned}\int_{\partial\Omega}\left(\frac{\partial u}{\partial \eta}\phi_4 - \frac{\partial \phi_4}{\partial \eta}u\right)ds &= \int_{\partial\Omega}\left(-\sqrt{\lambda}g(v)u\phi_4 - \left(\sigma_4 - \sqrt{\lambda}g(\epsilon)\right)\phi_4 u\right)ds\\ &= \int_{\partial\Omega}\phi_4 u\left(-\sigma_4 + \sqrt{\lambda}\left[g(\epsilon) - g(v)\right]\right)ds\\ &< \int_{\partial\Omega}\phi_4 u\left(-\sigma_4 + \sqrt{\lambda}\left[g(\epsilon) - g(\tilde{w}_2)\right]\right)ds < 0.\end{aligned}$$

This leads to a contradiction, and hence (1.3) has no positive solution in $\left[\lambda^{0,1}, \lambda^{0,1} + \xi_4\right]$.

5. Discussion

Consistent with the results in [22, 23], our mathematical analysis of (1.3) demonstrates that trait–mediated dispersal can impact the coexistence of interacting species, both in a competitive and in a predator–prey context. Since our modeling framework assumed density–mediated effects to be negligible, the interesting phenomena observed were due solely to trait–mediated dispersal. In both competition and predator–prey contexts, our results were highly dependent upon the patch size and effective matrix hostility. The model predicted that for sufficiently large patch sizes, coexistence is always predicted. This prediction is consistent with the ecological idea of a sufficiently large patch core area relieving enough of the mortality caused by organisms located outside of the core encountering the hostile matrix [17]. More interestingly, though, the model's predictions suggest that the most interesting dynamic scenarios occur for small to intermediate sized patches, which are precisely the size range of remnant patches resulting from habitat loss and fragmentation. Thus, as habitat loss and fragmentation increase, these results support the novel prediction that trait–mediated dispersal effects will become more frequent and pronounced.

In the competitive context, the competitor with the smaller MPS requirement had a competitive advantage and was able to competitively exclude its competitor for a range of patch sizes that included some patches where the competitor would be able to colonize an empty patch when alone. We also found interesting scenarios where a priority effect (or founder control) implied that for a range of patch sizes, the competitor that first colonized the patch was predicted to resist invasion from its competitor. Priority effects are generally thought to arise from the preemption of resources [35], but our models suggest that it can also arise from the resident species inducing greater emigration into the hostile matrix by its competitor. The model also predicted other ranges of patch size where a novel bistability between a coexistence state and a semi–trivial state implied that if one competitor could colonize the patch first, then it could resist invasion from its competitor, but if the other competitor colonized the patch first, then invasion by the other competitor was always possible, leading to coexistence.

In the predator–prey context, whenever the predator had the smaller MPS requirement, the model predicted the existence of a range of patch sizes where the prey could colonize an empty patch, but invasion by the predator would lead to the prey's extinction in the patch. When the prey had the smaller MPS requirement, certain parameter ranges yielded a range of patch sizes where a patch that would not be able to support the predator when alone would be able to support the predator as long as the prey was already established and near its steady–state. In this case, facilitation effects were observed, based solely upon the trait–mediated dispersal mechanism. Finally, when the predator and prey had the same MPS requirement, there were parameter ranges where coexistence was predicted for patches with a size greater than the MPS requirement. In this case, neither facilitation effects nor trait–mediated exclusion were predicted.

From a conservation point of view, these results greatly support the need for more careful consideration of trait–mediated effects in conservation efforts. According to our results, an endangered species in a trait–mediated dispersal relationship with an unknown second species can set up situations that could make conservation a challenge. For example, in the competitive context, if the endangered species is in one of the scenarios where the model predicted priority effects, then the situation could arise where a remnant patch has both competitors coexisting. However, if a stochastic event caused local extinction of the endangered species, then the system would flow towards the

stable semi–trivial state, implying that reintroduction of the endangered species would be impossible for low density levels. In the predator–prey context, if an endangered species is attracted to another species such that a facilitation effect occurs, then the endangered species is precariously dependent upon the facilitator species' presence in the patch to prevent local extinction.

Use of AI tools declaration

The authors declare they have not used artificial intelligence (AI) tools in the creation of this article.

Acknowledgments

This work is supported through the National Science Foundation under Grant No. DMS-2150945, DMS-2150946, DMS-2150947, DMS-2246723, DMS-2246724, and DMS-2246725.

Conflict of interest

All authors declare no conflicts of interest in this paper.

References

1. E. E. Werner, S. D. Peacor, A review of trait–mediated indirect interactions in ecological communities, *Ecology*, **84** (2003), 1083–1100. https://doi.org/10.1890/0012-9658(2003)084[1083:AROTII]2.0.CO;2
2. T. Ohgushi, O. Schmitz, R. D. Holt, *Trait–Mediated Indirect Interactions: Ecological and Evolutionary Perspectives*, Cambridge University Press, New York, 2012.
3. R. E. Irwin, *The Role of Trait-Mediated Indirect Interactions for Multispecies Plant-Animal Mutualisms*, Cambridge University Press, Cambridge, New York, (2012), 257–277.
4. A. P. Beckerman, M. Uriarte, O. J. Schmitz, Experimental evidence for a behavior-mediated trophic cascade in a terrestrial food chain (herbivore-mediated effects, predation, old field food chains, grasshoppers), *Proc. Natl. Acad. Sci. U.S.A.*, **94** (1997), 10735–10738. https://doi.org/10.1073/pnas.94.20.10735
5. E. M. Brice, E. J. Larsen, D. R. Stahler, D. R. MacNulty, The primacy of density–mediated indirect effects in a community of wolves, elk, and aspen, *Ecol. Monogr.*, **95** (2025), e1627. https://doi.org/10.1002/ecm.1627
6. R. D. Holt, M. Barfield, *Trait–Mediated Effects, Density Dependence and the Dynamic Stability of Ecological Systems*, Cambridge University Press, Cambridge, New York, 2012.
7. R. S. Cantrell, C. Cosner, Effects of harvesting mediated by dispersal traits, *Nat. Resour. Model.*, **31** (2018), e12168.
8. J. T. Cronin, K. J. Haynes, F. Dillemuth, Spider effects on planthopper mortality, dispersal, and spatial population dynamics, *Ecology*, **85** (2004), 2134–2143. https://doi.org/10.1890/03-0591
9. A. Sih, L. B. Kats, R. D. Moore, Effects of predatory sunfish on the density, drift, and refuge use of stream salamander larvae, *Ecology*, **73** (1992), 1418–1430. https://doi.org/10.2307/1940687

10. H. Hakkarainen, P. Ilmonen, V. Koivunen, E. Korpimäki, Experimental increase of predation risk induces breeding dispersal of Tengmalm's owl, *Oecologia*, **126** (2001), 355–359. https://doi.org/10.1007/s004420000525

11. B. L. Peckarsky, Alternative predator avoidance syndromes of stream-dwelling mayfly larvae, *Ecology*, **77** (1996), 1888–1905. https://doi.org/10.2307/2265793

12. E. O. Wilson, Threats to biodiversity, *Sci. Am.*, **261** (1989), 108–117. https://doi.org/10.1038/scientificamerican0989-108

13. I. Hanski, Habitat loss, the dynamics of biodiversity, and a perspective on conservation, *AMBIO*, **40** (2011), 248–255. https://doi.org/10.1007/s13280-011-0147-3

14. D. Tilman, M. Clark, D. R. Williams, K. Kimmel, S. Polasky, C. Packer, Future threats to biodiversity and pathways to their prevention, *Nature*, **546** (2017), 73–81. https://doi.org/10.1038/nature22900

15. K. J. J. Kuipers, J. P. Hilbers, J. Garcia-Ulloa, B. J. Graae, R. May, F. Verones, et al., Habitat fragmentation amplifies threats from habitat loss to mammal diversity across the world's terrestrial ecoregions, *One Earth*, **4** (2021), 1505–1513. https://doi.org/10.1016/j.oneear.2021.09.005

16. L. Ries, R. J. Fletcher Jr., J. Battin, T. D. Sisk, Ecological responses to habitat edges: Mechanisms, models, and variability explained, *Annu. Rev. Ecol. Evol. Syst.*, **35** (2004), 491–522. https://doi.org/10.1146/annurev.ecolsys.35.112202.130148

17. W. F. Fagan, R. S. Cantrell, C. Cosner, How habitat edges change species interactions, *Am. Nat.*, **153** (1999), 165–182.

18. R. S. Cantrell, C. Cosner, W. F. Fagan, Competitive reversals inside ecological reserves: the role of external habitat degradation, *J. Math. Biol.*, **37** (1998), 491–533. https://doi.org/10.1007/s002850050139

19. R. S. Cantrell, C. Cosner, Y. Lou, Multiple reversals of competitive dominance in ecological reserves via external habitat degradation, *J. Dyn. Differ. Equations*, **16** (2004), 973–1010. https://doi.org/10.1007/s10884-004-7831-y

20. A. Acharya, S. Bandyopadhyay, J. T. Cronin, J. Goddard, A. Muthunayake, R. Shivaji, The diffusive Lotka–Volterra competition model in fragmented patches I: Coexistence, *Nonlinear Anal. Real World Appl.*, **70** (2023), 103775. https://doi.org/10.1016/j.nonrwa.2022.103775

21. R. Harman, J. Goddard II, R. Shivaji, J. T. Cronin, Frequency of occurrence and population-dynamic consequences of different forms of density-dependent emigration, *Am. Nat.*, **195** (2020), 851–867. https://doi.org/10.1086/708156

22. J. T. Cronin, J. Goddard II, A. Muthunayake, R. Shivaji, Modeling the effects of trait–mediated dispersal on coexistence of mutualists, *Math. Biosci. Eng.*, **17** (2020), 7838–7861. https://doi.org/10.3934/mbe.2020399

23. J. T. Cronin, J. Goddard II, A. Muthunayake, J. Quiroa, R. Shivaji, Predator–induced prey dispersal can cause hump-shaped density-area relationships in prey populations, *J. Math. Biol.*, **88** (2024), 1–31. https://doi.org/10.1007/s00285-023-02040-1

24. J. T. Cronin, J. Goddard II, R. Shivaji, Effects of patch matrix-composition and individual movement response on population persistence at the patch-level, *Bull. Math. Biol.*, **81** (2019), 3933–3975. https://doi.org/10.1007/s11538-019-00634-9

25. N. Fonseka, J. Goddard II, Q. Morris, R. Shivaji, B. Son, On the effects of the exterior matrix hostility and a U-shaped density dependent dispersal on a diffusive logistic growth model, *Discrete Contin. Dyn. Syst. - Ser. S*, **13** (2020). https://doi.org/10.3934/dcdss.2020245

26. J. T. Cronin, N. Fonseka, J. Goddard II, J. Leonard, R. Shivaji, Modeling the effects of density dependent emigration, weak Allee effects, and matrix hostility on patch-level population persistence, *Math. Biosci. Eng.*, **17** (2019), 1718–1742. https://doi.org/10.3934/mbe.2020090

27. N. Fonseka, J. Goddard II, R. Shivaji, B. Son, A diffusive weak Allee effect model with U-shaped emigration and matrix hostility, *Discrete Contin. Dyn. Syst. - Ser. B*, **26** (2020), 5509–5517. https://doi.org/10.3934/dcdsb.2020356

28. A. Acharya, N. Fonseka, J. Goddard II, A. Henderson, R. Shivaji, On the effects of density-dependent emigration on ecological models with logistic and weak Allee type growth terms, *Discrete Contin. Dyn. Syst. - Ser. B*, **29** (2024), 1501–1524. https://doi.org/10.3934/dcdsb.2023142

29. A. Acharya, J. T. Cronin, N. Fonseka, J. Goddard II, A. Henderson, V. Munoz, et al., A Σ-shaped bifurcation curve for a class of reaction diffusion equations and an application to an ecological model, *Numer. Algebra, Control Optim.*, **2024** (2024), 1–17. https://doi.org/10.3934/naco.2024051

30. J. T. Cronin, N. Fonseka, J. Goddard II, R. Shivaji, X. Xue, Effects of predation-induced emigration on a landscape ecological model, *Axioms*, **14** (2025), 63. https://doi.org/10.3390/axioms14010063

31. J. Goddard II, Q. Morris, S. Robinson, R. Shivaji, An exact bifurcation diagram for a reaction diffusion equation arising in population dynamics, *Boundary Value Probl.*, **170** (2018), 1–17. https://doi.org/10.1186/s13661-018-1090-z

32. R. S. Cantrell, C. Cosner, *Spatial Ecology via Reaction-Diffusion Equations*, Mathematical and Computational Biology. Wiley, Chichester, 2003.

33. C. V. Pao, *Nonlinear Parabolic and Elliptic Equations*, Plenum Press, New York, 1992.

34. T. Laetsch, The number of solutions of a nonlinear two point boundary value problem, *Indiana Univ. Math. J.*, **20** (1970), 1–13.

35. T. Fukami, Historical contingency in community assembly: Integrating niches, species pools, and priority effects, *Annu. Rev. Ecol. Evol. Syst.*, **46** (2015), 1–23. https://doi.org/10.1146/annurev-ecolsys-110411-160340

Appendix

In this appendix, we provide a proof of the quadrature method Theorem 3.1.

Proof of Theorem 3.1

First, suppose (u, v) is a positive solution to (3.5). It follows easily to note that unique values $x_u^*, x_v^* \in (0, 1)$ exist such that u is increasing on $(0, x_u^*)$, u is decreasing on $(x_u^*, 1)$, v is increasing on $(0, x_v^*)$, and v is decreasing on $(x_v^*, 1)$ (see Figure 20). If we multiply the first equation of (3.5) by u',

we have

$$-\left(\frac{[u']^2}{2}\right)'(x) = \lambda[F(u)]'(x).$$

This implies

$$u'(x) = \begin{cases} \sqrt{2\lambda[F(\rho_u) - F(u(x))]} & x \in (0, x_u^*) \\ -\sqrt{2\lambda[F(\rho_u) - F(u(x))]} & x \in (x_u^*, 1). \end{cases}$$

It follows that

$$\sqrt{2\lambda}x = \int_{u(0)}^{u(x)} \frac{ds}{\sqrt{F(\rho_u) - F(s)}};\ x \in (0, x_u^*)$$
$$\sqrt{2\lambda}(1-x) = \int_{u(1)}^{u(x)} \frac{ds}{\sqrt{F(\rho_u) - F(s)}};\ x \in (x_u^*, 1).$$

Letting $x \to x_u^*$ with $u(x_u^*) = \rho_u$, we have

$$\sqrt{2\lambda}x_u^* = \int_{u(0)}^{\rho_u} \frac{ds}{\sqrt{F(\rho_u) - F(s)}}$$
$$\sqrt{2\lambda}(1-x_u^*) = \int_{u(1)}^{\rho_u} \frac{ds}{\sqrt{F(\rho_u) - F(s)}}.$$

From these two equations, we obtain:

$$\sqrt{2\lambda} = \int_{u(0)}^{\rho_u} \frac{ds}{\sqrt{F(\rho_u) - F(s)}} + \int_{u(1)}^{\rho_u} \frac{ds}{\sqrt{F(\rho_u) - F(s)}} \tag{5.1}$$

$$x_u^* = \frac{\displaystyle\int_{u(0)}^{\rho_u} \frac{ds}{\sqrt{F(\rho_u) - F(s)}}}{\displaystyle\int_{u(0)}^{\rho_u} \frac{ds}{\sqrt{F(\rho_u) - F(s)}} + \int_{u(1)}^{\rho_u} \frac{ds}{\sqrt{F(\rho_u) - F(s)}}}. \tag{5.2}$$

Similar calculations apply to the second equation of (3.5) yielding:

$$\sqrt{2\lambda} = \int_{v(0)}^{\rho_v} \frac{ds}{\sqrt{r[F(\rho_v) - F(s)]}} + \int_{v(1)}^{\rho_v} \frac{ds}{\sqrt{r[F(\rho_v) - F(s)]}} \tag{5.3}$$

$$x_v^* = \frac{\displaystyle\int_{v(0)}^{\rho_v} \frac{ds}{\sqrt{r[F(\rho_v) - F(s)]}}}{\displaystyle\int_{v(0)}^{\rho_v} \frac{ds}{\sqrt{r[F(\rho_v) - F(s)]}} + \int_{v(1)}^{\rho_v} \frac{ds}{\sqrt{r[F(\rho_v) - F(s)]}}}. \tag{5.4}$$

By the boundary condition $u'(0) = \sqrt{\lambda}g(v(0))u(0)$ and using the above analysis, we have

$$u'(0) = \sqrt{2\lambda[F(\rho_u) - F(u(0))]},$$

it follows that

$$[g(v(0))u(0)]^2 = 2[F(\rho_u) - F(u(0))].$$

Using similar calculations and making use of the boundary conditions, the last three equations in (3.6) follow.

For the reverse direction, assume that $\lambda, q_1(:= u(0)), q_2(:= u(1)), q_3(:= v(0)), q_4(:= v(1)), \rho_u,$ and ρ_v with $0 < q_1, q_2 < \rho_u$, and $0 < q_3, q_4 < \rho_v$ satisfy (3.6). Let

$$x_u^* = \frac{\displaystyle\int_{q_1}^{\rho_u} \frac{ds}{\sqrt{F(\rho_u) - F(s)}}}{\displaystyle\int_{q_1}^{\rho_u} \frac{ds}{\sqrt{F(\rho_u) - F(s)}} + \int_{q_2}^{\rho_u} \frac{ds}{\sqrt{F(\rho_u) - F(s)}}}$$

and

$$x_v^* = \frac{\displaystyle\int_{q_3}^{\rho_v} \frac{ds}{\sqrt{r[F(\rho_v) - F(s)]}}}{\displaystyle\int_{q_3}^{\rho_v} \frac{ds}{\sqrt{r[F(\rho_v) - F(s)]}} + \int_{q_4}^{\rho_v} \frac{ds}{\sqrt{r[F(\rho_v) - F(s)]}}}.$$

Define $(u, v) : [0, x_u^*) \times [0, x_v^*) \to [q_1, \rho_u) \times [q_3, \rho_v)$ such that $u(x)$ satisfies:

$$\sqrt{2\lambda}x = \int_{q_1}^{u} \frac{ds}{\sqrt{F(\rho_u) - F(s)}};\ x \in (0, x_u^*) \tag{5.5}$$

and $v(x)$ satisfies:

$$\sqrt{2\lambda}x = \int_{q_3}^{v} \frac{ds}{\sqrt{r[F(\rho_v) - F(s)]}};\ x \in (0, x_v^*). \tag{5.6}$$

Note that $\sqrt{2\lambda}x$ is increasing for $x \in (0, x_u^*)$ with the range $(0,\ \sqrt{2\lambda}x_u^*) = \left(0, \displaystyle\int_{q_1}^{\rho_u} \frac{ds}{\sqrt{F(\rho_u) - F(s)]}}\right)$, while $\displaystyle\int_{q_1}^{u} \frac{ds}{\sqrt{F(\rho_u) - F(s)}}$ is also an increasing function of u on (q_1, ρ_u) with the same range. Hence, u is well-defined on $[0, x_u^*)$, and a similar analysis shows that v is well-defined on $[0, x_v^*)$.

Next, define $H_u : [(0, x_u^*) \times (q_1, \rho_u)] \to \mathbb{R}$ and $H_v : [(0, x_v^*) \times (q_3, \rho_v)] \to \mathbb{R}$ by

$$\begin{cases} H_u(\ell, w) := \sqrt{2\lambda}\ell - \displaystyle\int_{q_1}^{w} \frac{dz}{\sqrt{F(\rho_u) - F(z)}} \\ H_v(m, y) := \sqrt{2\lambda}m - \displaystyle\int_{q_3}^{y} \frac{dz}{\sqrt{r[F(\rho_v) - F(z)]}}. \end{cases}$$

Then H_u and H_v are C^1 with $H_u(x, u) = H_v(x, v) = 0$, while $(H_u)_w(0, u) \neq 0$ and $(H_v)_y(0, v) \neq 0$. Hence by the implicit function theorem, u and v defined above are C^1 functions on $(0, x_u^*)$ and $(0, x_v^*)$, respectively, and by differentiating (5.5) and (5.6), we easily see that they are, in fact, C^2 functions on $(0, x_u^*)$ and $(0, x_v^*)$ satisfying $-u'' = \lambda f(u);\ (0, x_u^*)$ and $-v'' = \lambda r f(v);\ (0, x_v^*)$, respectively. Note that $u(0) = q_1$ and $v(0) = q_3$. Furthermore, (5.5) and (5.6) imply that the third and fifth equations of (3.5) are satisfied.

Similarly, we can define u and v on $(x_u^*, 1]$ and $(x_v^*, 1]$ as

$$\sqrt{2\lambda}(1-x) = \int_{q_2}^{u} \frac{ds}{\sqrt{F(\rho_u) - F(s)}};\ (x_u^*, 1] \tag{5.7}$$

$$\sqrt{2\lambda}(1-x) = \int_{q_4}^{v} \frac{ds}{\sqrt{r[F(\rho_v) - F(s)]}};\ (x_v^*, 1] \tag{5.8}$$

and obtain the C^2 functions satisfying $-u'' = \lambda f(u);\ (x_u^*, 1)$ and $-v'' = \lambda r f(v);\ (x_v^*, 1)$ with $u(1) = q_2$ and $v(1) = q_4$. Again, (5.7) and (5.8) imply that the fourth and sixth equations in (3.5) are satisfied. Finally, define $u(x_u^*) = \rho_u$ and $v(x_v^*) = \rho_v$. It is easy to see that these functions are, in fact, C^2 on $(0, 1)$ and will satisfy (3.5).

AIMS Press